Goodbye Andromeda?

Galaxy collision simulation of the effect of the transverse velocity component on the evolution of the Milky Way Andromeda system

by

Edda Heinsman

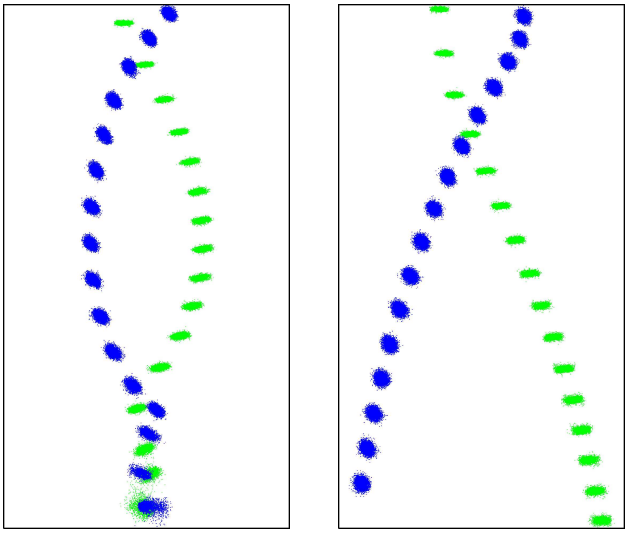

Supervised by dr. S.F. Portegies Zwart and dr. S. Harfst

Universiteit van Amsterdam

The University of Amsterdam

Faculty of Science

Astronomical Institute "Anton Pannekoek"

June 2007 - March 2008

KEYWORDS: N-BODY SIMULATION, GALAXY COLLISION, ANDROMEDA, MILKY WAY, TRANSVERSE VELOCITY, GPU

Cover image: Two possible futures for the Milky Way Andromeda system. Left image is a hit, right image is a miss. Timescale is 4 Billion years to 10 Billion years from now.

Preface

This thesis covers the work done during my master's research project as part of the fulfillment of the master's degree in Astronomy and Astrophysics (M-profile) at the University of Amsterdam. This research project is done under the supervision of dr. S.F. Portegies Zwart and dr. S. Harfst at the Astronomical Institute "Anton Pannekoek" from June 2007 until March 2008.

Abstract

Andromeda (M31) and the Milky Way (MW) approach each other with 117 km/s, so a giant collision seems inevitable. But the transverse velocity component is unknown. Therefore there could be a chance they will not collide. We investigate that possibility by performing N-body simulations of the merger between M31 and the MW using a GPU enabled treecode.
To find the initial conditions of the system we perform a literature study, and find out that for mass, transverse velocity and radius, there is a wide variety of estimates.
We use Kuijken and Dubinski models (Kuijken and Dubinski, 1995) to create galaxies with a disk, bulge and dark matter halo. To make sure the galaxies are stable, we create galaxies with different numbers of halo particles and choose the model that, based on energy conservation and disk thickness, stays stable over a considerable timescale.
We run our simulations with the GPU enabled treecode and two other codes. By comparing their performance we conclude that the GPU is a good device to use for these simulations (energy error $\sim 1/1000$ and computation time about 6 hours for 500 time evaluations).

We create a M31-MW model with several initial transverse velocities (v_t), with as a maximum the value where the galaxies become unbound (v_t=171 km/s). We conclude that for a total mass for both galaxies of $3.9 \times 10^{12} M_{\odot}$ the galaxies will merge within 10 Gyr if v_t <86 km/s. The collision will happen earliest at 3.4 Gyr from now, for (v_t)=0. The merging galaxies result in an elliptical galaxy and the shape of this merger depends on the initial transverse velocity.
If the transverse velocity exceeds 171 km/s, there will be no merger at all.

Contents

1 Introduction **1**

2 Formation and currently observed Galaxies **3**
2.1 Evolution 3
2.1.1 Hierarchical/ΛCDM aggregation 4
2.2 Types of Galaxies 5
2.3 Components of the Milky Way 8
2.4 Measured/observed parameters Milky Way vs Andromeda . . 12
2.4.1 Historical overview 12
2.4.2 Orientation Spin Axis 14
2.4.3 Distance and Position 14
2.4.4 Extent / Radius 14
2.4.5 Begin Velocities 15
2.4.6 Mass 17
2.4.7 First approach vs. transverse velocity 19

3 Methods **23**
3.1 N-body modelling 23
3.2 Time scales 23
3.3 Algorithms 24
3.4 Choice of code 25

4 Set up galaxies **34**
4.1 Creating K&D-galaxies 34
4.2 Set up merger model 36
4.2.1 Orientation 36
4.2.2 Distance, position and velocities 38

5 Results **40**
5.1 Collision probability 40
5.2 Structure after collision 44
5.3 Location of the Sun 47

6 Discussion and Recommendations **50**
6.1 Milkomeda? 50
6.2 Future research 50
6.3 Concerning work process 52

7 Conclusions **54**

Bibliography **55**

A Input parameters **58**

B Coordinates **58**

C Paper by Widrow et al. **58**

1 Introduction

Why is it so important to investigate the behavior of galaxies? According to Binney and Tremaine (1987) the studies of galaxies can answer questions about the formation of the early universe and about dark matter. Galaxies can be looked at as giant laboratories, their dazzling properties so extreme they can not be compared to anything earthly. However, it is possible to simulate these conditions and create virtual galaxies that resemble the ones we can observe every cloudless night.

Many astrophysicists try to answer this question. Smarter calculation methods and increasing computational capabilities made it possible to perform huge N-body simulations. The Graphics Processing Unit (GPU) Portegies Zwart et al. (2007) offers an interesting new device for calculating particle interactions, where high precision is not necessary. The GPU has a theoretical peak performance of about 500 GFLOP/s (500 billion floating-point operations per second) which is about 50 times faster than a regular computer. Practically the GPU is about twenty times faster than the normal computer.
Many simulations have been done to get more knowledge about the distribution and nature of dark matter (DM). Telescopes can only look so far, and even if they could look farther, DM could not be detected. With the *theoretical telescope* that computational astrophysics provides, one can not only look into the past, but also in the future. With this research we want to find out what the future brings for our own galaxy.
Since the Andromeda galaxy is currently observed to approach our Milky Way with a velocity of more then 100 km/s, a giant collision seems inevitable. But the transverse velocity component of M31 is not so well known. So could there be a chance there will be no merger, and in fact we have to say **Goodbye Andromeda?**

The goal of this research is to answer the following questions:

- **How probable is it that the Milky Way and Andromeda[1] will collide?**
- Where will the Sun be during the collision?
- What happens to the structure of Milkomeda (merger between the Milky Way and Andromeda)?
- Will Milkomeda be comparable to any object that is currently observed?

[1] Andromeda is also known as M31, short of Messier-31, number 31 of 109 nebulae in Charles Messiers catalogue (1784), and as NGC 224, number 224 in John Dreyers' New General Catologue of Nebulae and Clusters of Stars.

- Is the GPU a good device for these kind of calculations?

To answer the above questions we will start in chapter 2 with a short literature study about the cosmological evolution of the local group. In this chapter we will also make a comparison between Andromeda and our Galaxy, based on the literature.

In chapter 3 we will give an introduction to our used methods. We describe the most essential steps that have to be taken for N-body simulations. We also give an overview of the three different codes we used and how they perform.

In chapter 4 we describe how stable galaxies can be simulated with the method presented by Kuijken and Dubinski (1995) (K&D-method). Furthermore we describe the initial conditions we use for the simulations.

We run the models with our initial conditions, the results can be read in chapter 5.

We compare our results with Kuijken and Dubinski (1995), Dubinski et al. (1996) and Cox and Loeb (2007) in chapter 6. Here we also describe the limitations of our used models and the initial conditions. And we give an overview of interesting future research.

In the chapter 'Conclusions' we summarize our main conclusions.

2 Formation and currently observed Galaxies

To say something about the future evolution of galaxies, it is necessary to first know more about the formation of galaxies, and galaxies in general. In the first section we give an introduction to the possible formation scenario, a short overview of different types of galaxies and the components of the Milky Way. In the second section we explain some measured parameters that describe Andromeda and the Milky Way.

2.1 Evolution

According to Binney and Tremaine (1987) there is no widely accepted theory for galaxy formation, but more recent studies give a strong favour for the Hierarchical/ΛCDM aggregation model for the growth of galaxies (see next paragraph). Cosmologists do agree that after the big bang the universe existed fully of hot plasma (mixture of atomic nuclei, photons and electrons), 'like the inside of a fluorescent light' (Sparke and Gallager, 2000) . The universe kept expanding and cooling. About 380000 years after the big bang, when the universe was cooled to $\sim$3000 K, the electrons and protons could combine to form hydrogen atoms (recombination). The free electrons were captured so the universe became less dense, which gave photons the opportunity to travel more freely (decoupling). Theory by Gamow, Alpher and Herman (1948) predicted we still should be able to see these free photons, though they should be cooled a lot. In 1965, Penzias and Wilson were the first to measure the microwave background radiation (CMB).
The CMB is not homogeneously distributed, small perturbations can be seen. The theory is that these tiny perturbations in density structure could grow because of their gravitational attraction, and because the photons escaped, their pressure no longer prevented this from happening. The more dense parts kept getting denser until density (after about 200 million years) was so high that stars could form (perturbations with a scale larger than the Jeans-length cause star formation): the birth of the first protogalaxies. The period between the moment of recombination and the formation of the first stars is known as the 'Dark Ages', because there were no sources of light in the universe. Figure 1 gives a schematic overview of the evolution of the universe.
The Hubble Ultra Deep Field Survey (2004) created visible-light images of the universe when it was only about 0.7 Billion years old (13 Billion years ago). The images show the first proto galaxies, made of gas and dark matter and of sizes comparable to dwarf galaxies. The GEMS survey (2004) looks back 9 Billion years and observes the first spiral galaxies.

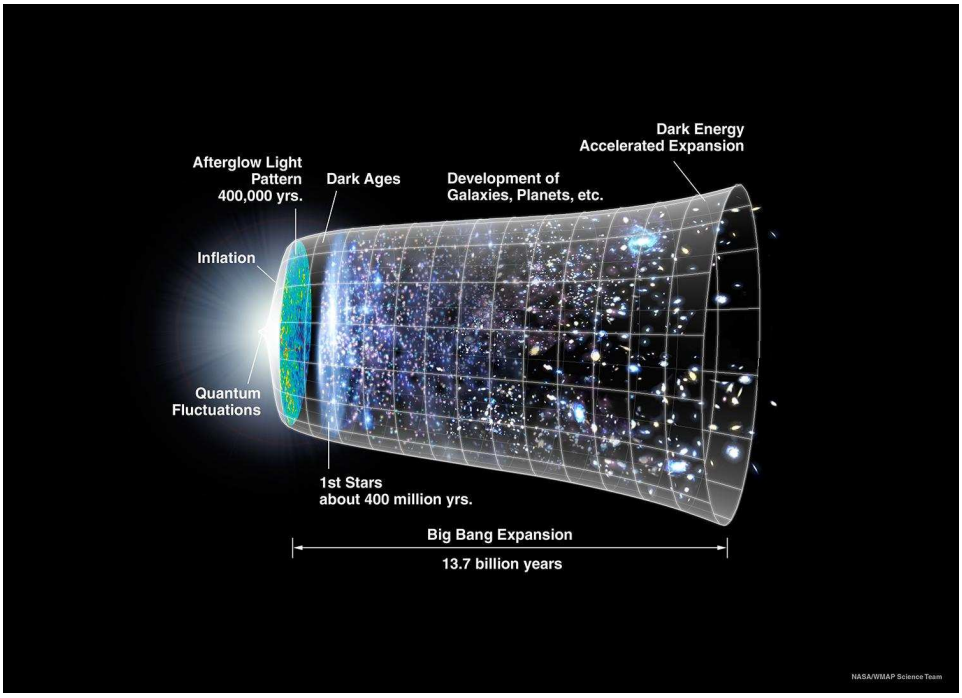

Figure 1: Evolution of the universe. *credit: NASA/WMAP Science team*

2.1.1 Hierarchical/ΛCDM aggregation

How exactly the first perturbations could grow large enough to evolve into galaxies is unknown. There are two main theories about galaxy formation: the Cold Dark Matter theory (also referred to as hierarchical or bottom-up model) and the Hot Dark Matter theory (Freeman and Bland-Hawthorn, 2002). 'Hot' and 'cold' refer to the velocity of the dark matter particles: ultrarelativistic for HDM and not relativistic for CDM. HDM theory predicts that the initial perturbations can only grow out to massive objects on the scale of a cluster of galaxies. In this manner large scale structures evolve very fast Freeman and Bland-Hawthorn (2002). CDM predicts that also regions of low masses can collapse to form stars. With this model, we can better explain the existence of very old stars. Comparing HDM evolution simulations with the current observations of the large scale structure shows to much substructure. CDM actually shows not enough substructure. The CDM theory is currently favoured over the HDM theory (Longair, 1998). CDM assumes that dark matter particles interact in the way baryonic matter does, their interactions depend on the gravitational force. The idea is that the initially formed low mass dark matter regions can grow due to clustering (bottom-up model). These massive structures attract also baryonic matter and so the first protogalaxies start to evolve.

The (evolution of the) distribution of dark matter is very important for the evolution of the universe. But since dark matter is dark, it can not be observed directly. The only (indirect) observations come from the kinematics of visible matter, from the lensing effect and from the existence of the CMB as described in the previous paragraph. In 1933 Zwicky compared the velocities of galaxy clusters to their lightcurves and found out that based on the kinematics the mass was higher than based on the received light, Zwicky was the first to use the term *Dark Matter*. Kahn and Woltjer in 1959 looked at the velocities of the local group and by assuming this is a bound system, they found a higher mass than could be explained by the visible matter. In the early eighties the flat rotation curves of galaxies gave even more proof that there exists more mass than we can observe.

Light bends while traveling through a potential, so (massive) distinct galaxies can work as giant lenses and bundle the light from distant sources, so we can observe it from earth. A recent paper by Clowe et al. (2007) claims to have found the first direct evidence for the existence of dark matter. Using the weak lensing effect of two merging clusters (1E0657-56, better known as the Bullet Cluster), they created a map of the dark matter in the system. Clowe et al. (2007) distinct three different components: the dark matter halo, galaxies (which contain about 10% of the visible cluster matter) and gas (about 90 %). The collision affects these components in a different manner, hereby providing information about the nature of these components. The gaseous component is highly collisional, so the plasma slows down during the merger (see figure 2, pink regions). The galaxies fly through each other and are only affected by tidal forces. The question of course is: What happens to the dark matter during the collision? If the dark matter behaves collisionless (as assumed by CDM), they follow the galaxies. Armed with their weak lensing maps, Clowe et al. (2007) conclude that the dark matter indeed follows the galaxies (see figure 2, blue regions).

Ostriker and Peebles (1973) tried to simulate a stable galactic disk and found out that a real stable disk needs a massive halo. Since spirals make up a large part of all Galactic systems in the local universe (they contain approximately 40 to 60% of the luminosity), these dark matter halos should be omnipresent.

2.2 Types of Galaxies

Galaxies are found in very different morphologies. Edwin Hubble was one of the first to classify the shapes of galaxies (Hubble, 1922). In his article 'A general study of diffuse galactic nebulae' Hubble recognized there are galactic and 'non-galactic' nebulae. He divided the extra galactic once in Spiral, Elongated (subclasses Spindle and Ovate), Globular and Irregular. His complete classification system (Hubble, 1926), where he distinguishes

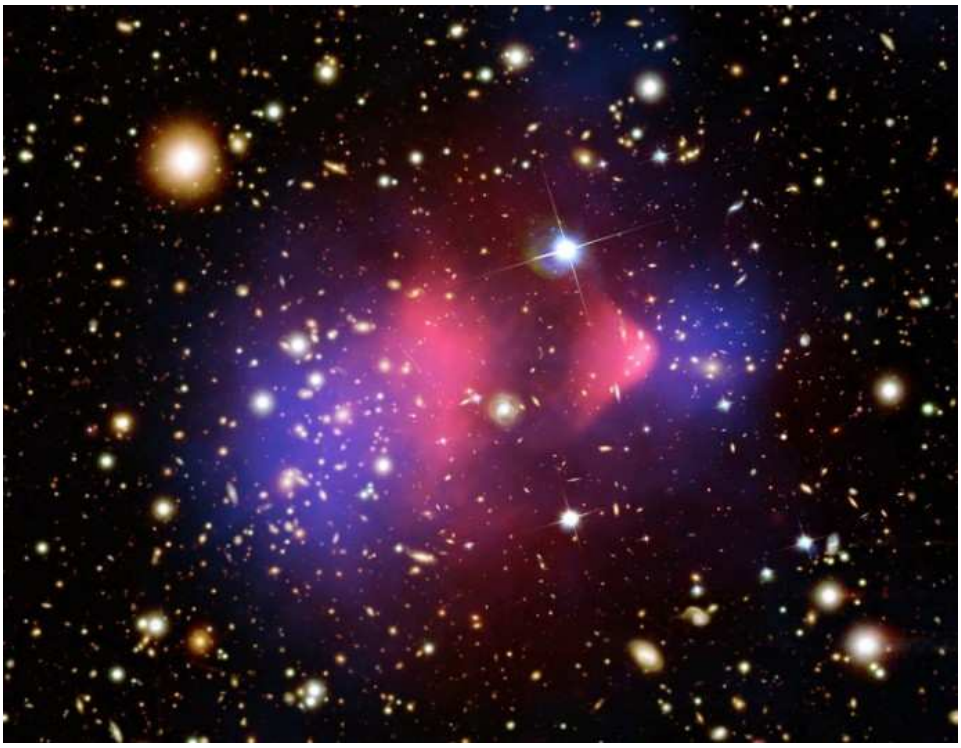

Figure 2: 1E 0657-56, the bullet cluster, hot gas in pink, dark matter in blue *credit: X-ray: NASA/CXC/CfA/ M.Markevitch et al.; Lensing Map: NASA/STScI; ESO WFI; Magellan/U.Arizona/ D.Clowe et al. Optical: NASA/STScI; Magellan/U.Arizona/D.Clowe et al.;*

elliptical (En, where n stands for the ellipticity) and spiral galaxies (S), barred spirals(SB), with subtypes early (a), intermediate (b) and late (c), is still used today. The Hubble-diagram gives merely an overview of the different shapes of galaxies, contrary to what Hubble ones thought (and why he called ellipticals 'early' and spirals 'late') it does not give the evolutionary track of a galaxy. One argument against Hubbles evolution model is that spirals have a high rotation velocity and this is not true for ellipticals. Since there is no reason for elliptical galaxies to start rotating, it is not likely that spirals evolve from ellipticals.
But it is true that the morphology of a galaxy contains information about how it is formed, more about this in this section. Because of its shape the scheme is also referred to as the Hubble Tuning-Fork diagram (see figure 3).

As we saw in the previous chapter, galaxies originate from dark matter and gas. But after this the galaxy is not complete yet. This is very different from stellar-evolution: a star comes into existence from the collision of a molecular cloud. The rest of its life its stays a star, since the chance that

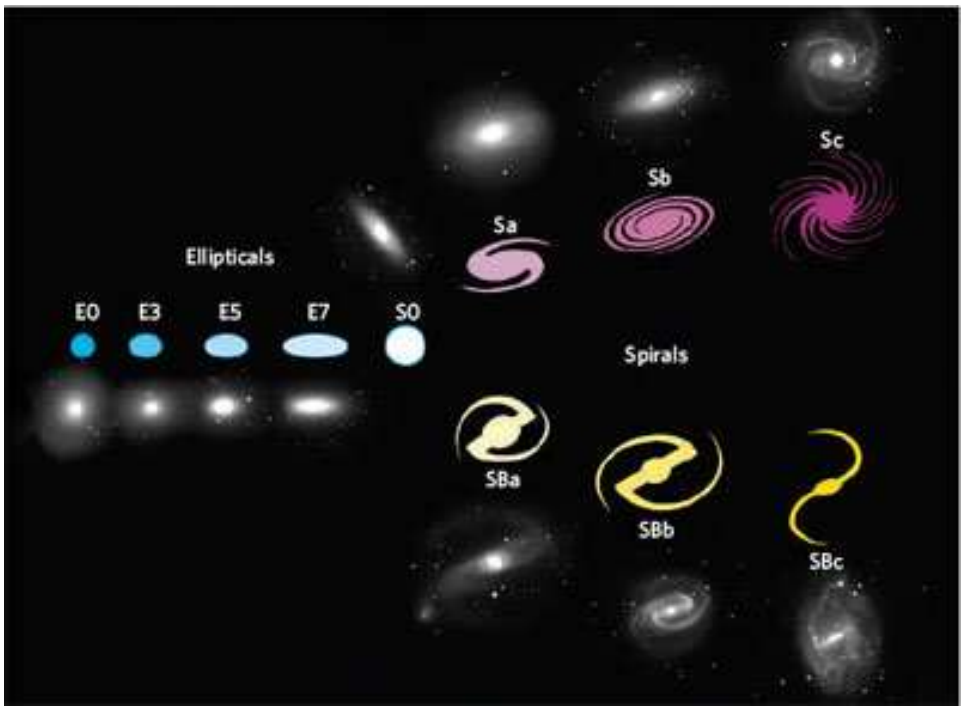

Figure 3: Hubble Tuning-Fork diagram. *credit: HubbleSite.org*

a star collides with another star is very small. The chance that a galaxy collides with another galaxy is very big.
In the next paragraphs we will discuss some properties of different galaxy types and how current theory explains their formation.

Dwarf
Dwarf galaxies have typically several billion stars and the smallest ones' luminosities are comparable to larger globular clusters. They contain less metal than is expected by their ages. Though their stellar density appears to be much lower than that of globular clusters, their random velocities are comparable. With the assumption of equilibrium (and the virial theorem) this leads to the idea that dwarf galaxies should contain a lot of dark matter (Sparke and Gallager, 2000).

Spiral
Andromeda and the Milky Way are spiral galaxies. They contain a disk of population 1 stars (population 1 means stars with solarlike metallicity, so young stars), gas and dust (Binney and Tremaine, 1987). They have spiral arms. These galaxies can be characterized by their shape and velocities. Stars in spirals have no mentionable velocity in the direction perpendicular to the plane. Their rotation curves are nearly flat, with exception of the

center.

Elliptical
It is currently believed that elliptical galaxies are the product of several merged (spiral) galaxies. A lot of ellipticals can be observed. More ellipticals are found at centres of the spiderweblike structures that you see on large scale, whereas the spirals are at the more outer parts. This agrees with the theory that when spirals collide they form ellipticals. Contrary to spiral galaxies, the rotation in the z-direction is not zero. That the collision of two spirals of the same mass results in an elliptical is also shown in simulations (e.g. Dubinski et al. (1996)). According to Murdin (2001) they are smooth and featureless and contain almost no gas or dust. At this moment some dwarf galaxies seem to be losing stars to the Milky Way, for instance Sagittarius (Sparke and Gallager, 2000). We are also interacting with the Small and Large Magellanic Clouds.

Peculiar
The 'irregular galaxies' actually seem to be in stage of collision. In 1977 Toomre participated in a conference about the evolution of galaxies and stellar populations. Here he spoke about eleven galaxy systems that he roughly ordered in range of 'completeness of the imagined mergers' (Tinsley and Larson, 1977).

2.3 Components of the Milky Way

In this subsection we will discuss the formation and some characteristics of the different components of the Milky Way. Figure 5 shows a near-infrared image of our own galaxy.

Disk
The disk exist mostly of young stars and almost all of the gas that is in the galaxy. It has a bar and spiral arms. How the spiral arms are formed is also not clear. Stars are moving through the spiral arms (differential rotation) so they must be a wave phenomenon. The discovery that our own galaxy has spiral arms is done by the detection of H2/21 cm radiation.

Bulge
The bulge is pretty young, it was created after the disk. According to (Murdin, 2001): *'A very plausible model of the formation of the galactic bulge has the majority of the stars form through the dissipative and violent collapse of protogalactic gas clouds in the first billion years of cosmic history. There is clear evidence, however, that the bulge has added to its stock of stars since that time. A number of processes, such as mergers of dwarf galaxies and disk instabilities, could be responsible for that extended population.'* In the

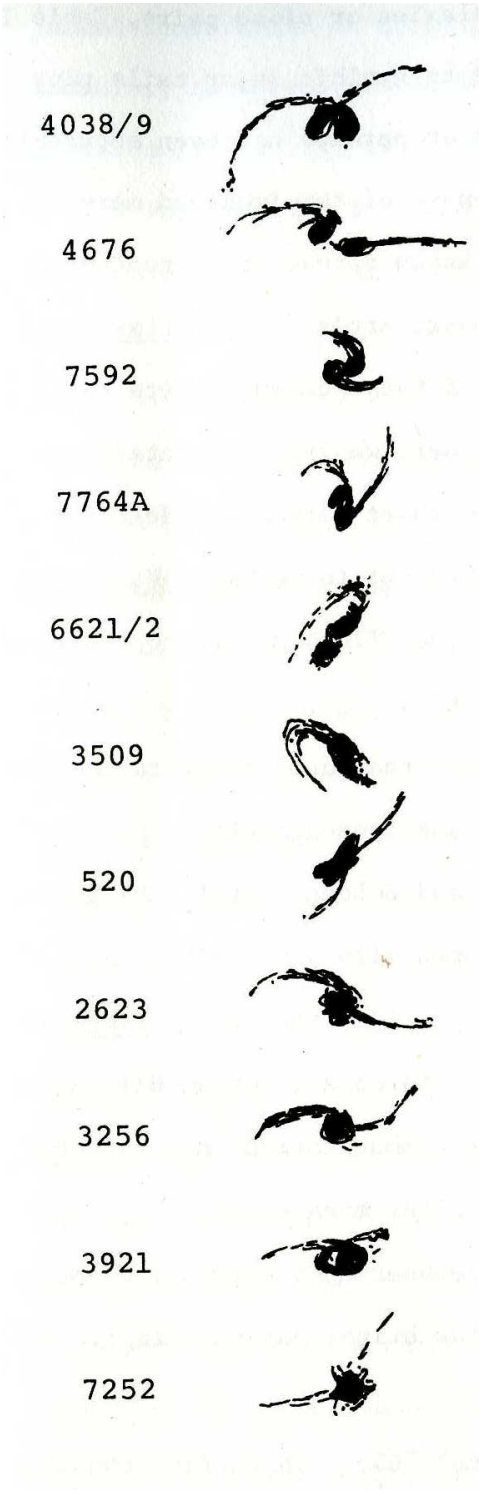

Figure 4: Toomre sequence: eleven observed merging galaxies. (Numbers refer to NGC). *credit: Tinsley and Larson (1977)*

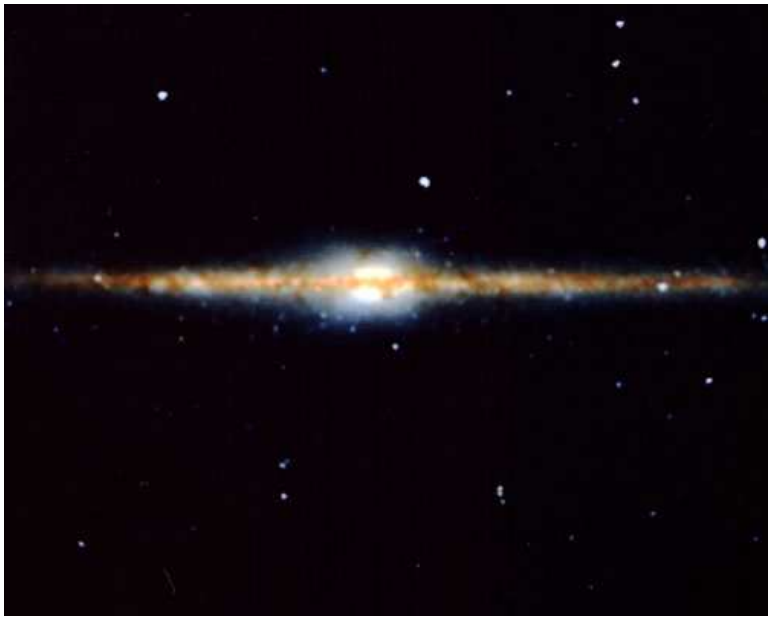

Figure 5: Milky Way near-infrared image. *credit: European Southern Observatory & NASA COBE Project.*

core of our galaxy we have a black hole of about 2.5 $10^6 M_\odot$.

Halo
The halo is spherical as well. Here we find the oldest stars and globular clusters. Globular clusters have a spherical distribution around the galactic centre. They contain the oldest stars and no gas, dust or young stars. They are spherical and contain about 10^4 to 10^6 stars.

Dark Halo
There are several observations that support the prediction of the existence of dark matter halos: the galactic dynamics and the gravitational lensing-effect of galaxies. One of the indicators of dark matter can be found in the timing argument (first mentioned by Kahn and Woltjer in 1959); since we see Andromeda and the Milky Way approaching each other, their gravitational attraction should exceed the cosmological expansion. But the mass we observe is not enough to cause this gravitational attraction, leading again to the idea of dark matter. Also, when looking at the rotation curve (figure 6), we seem to miss matter. The rotation curve goes straight for larger radii, where you expect it to go down, because of the decreasing number of visible matter.

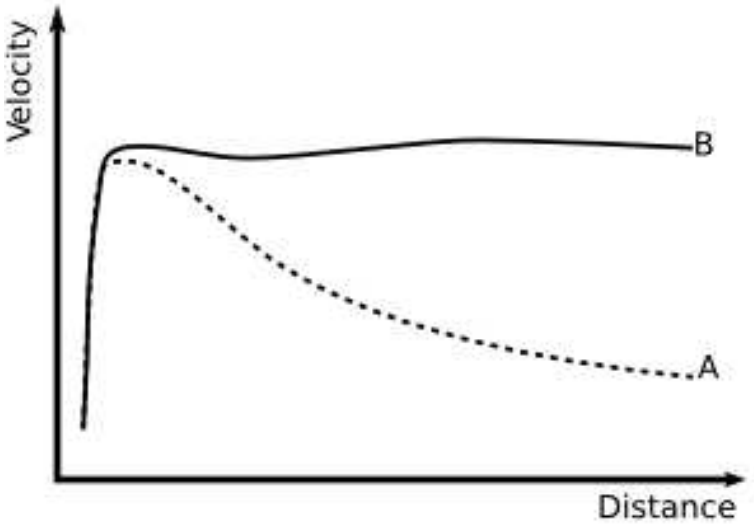

Figure 6: Expected rotation (A) and observed rotation (B).

2.4 Measured/observed parameters Milky Way vs Andromeda

Creating a Galaxy that is stable over several billion years, is not an easy task. In the following paragraphs we discuss the parameters that represent the Galaxy and Andromeda. We compare the different parameters used in literature and discuss the initial conditions Kuijken and Dubinski used (Kuijken and Dubinski, 1995). But first we give a short historical overview of the growing knowledge about the Galaxy and Andromeda.

2.4.1 Historical overview

Herschell was one of the first astronomers who tried to map the Galaxy. He counted the number of stars in different directions and the assumption that all stars are equally bright, gave him an idea about the their distances and therfor the shape of the Galaxy. Because Herschell did not know the distances to the stars, he could not estimate the extent of the Galaxy, but he did find an oval shaped model (Herschel, 1785).

Hugo von Seeliger (1849-1924) was slightly more succesful in 1898. He counted the number of stars with about the same magnitude, for increasing magnitude, and found the 'fundamental equation of stellar statistics', which, in a somewhat adjusted form, is still used today. His research lead to an ellipsoidal model of the Galaxy with a diameter of 3000 pc and thickness of 1300 pc (Murdin, 2001). In 1915 Eddington increased the estimation of the galactic diameter to about 4600 pc (Plaskett, 1932), and in 1920 Kapteyn even estimated the radius to be 5500 pc. Until then it was believed that the Sun was in the centre of the Galaxy. Interstellar absorption causes the effect that the star density seems to be dropping down at large radii, regardless of the direction in the galactic plane. Shapley derived a new method of estimating the scale of the Galaxy. He observed 11 variable stars (nowadays referred to as RR Lyrae stars) and used the relation Leavitt found in 1908 (the higher the total luminosity of the variable star, the longer the period of variation) to estimate the distance. With this method he determined the distances and locations of globular clusters and found they where not centered around the Sun. Shapley came to the conclusion that our Galaxy is about 100,000 pc in diameter and that the Sun is at one fifth of the centre.

Around the mid 1920s both Oort and Lindblad found evidence that the Galaxy is rotating, but Lindblad used a model based on a rotating rigid body. Oort looked at the actual velocities and found that in the Galactic centre the velocities were much higher, so he also discovered there is a large amount of mass in the centre. In Oorts model the Galaxy diameter is about a third of Shapley's and the distance between the Sun and the Galactic centre is about 6000 pc. In 1952, Baade found out there was an error in the period luminosity relationship and that all the calculated distances to other

Article	Distance(kpc)
Opik (1922)	450
Hubble (1929)	275
Gott and Thuan (1978)	700
Binney and Tremaine (1987)	730
Dubinski et al. (1996)	700
Sparke and Gallager (2000)	770
Evans and Wilkinson (2000)	770
Loeb et al. (2005)	786[1]
Koch and Grebel (2006)	773±20
Cox and Loeb (2007)	780[1]
Metz et al. (2007)	785[1]
van der Marel and Guhathakurta (2007)	770±40[1]

Table 1: Distances (from the Sun) to Andromeda

galaxies should be doubled, so the sizes of the galaxies should be doubled as well. At that time astronomers found out that the Galaxy was not twice as large as other galaxies.
The size is currently believed to be 25,000 - 30,000 parsec in diameter, about 300 pc thick (at the distance of the Sun) and our bulge is approximately 5 kpc thick. The Sun is located at about 8 kpc from the galactic centre.

In the beginning of the 20th century there was a great debate (appositely called 'The Great Debate') about the size of our Milky Way galaxy, and about whether the observed 'nebulae' were either part of our Galaxy, or if they were intergalactic. In the 1920's more and more observations were made that favoured the idea of the nebulae to be extragalactic. Hubble for instance compared in 1929 period-luminosity diagrams of Cepheids in M31 with the diagrams for the small Magellanic cloud and found that M31 is about 8.5 times more distant. With Shapley's value for the SMC he found a distance for Andromeda of 275 kiloparsec. Opik (1922) recognizes Andromeda (already in 1922) as a stellar universe, comparable with our own Galaxy. As you can see in table 1, both Hubble and Oepik found values for the distance to Andromeda that exceeded the at that time assumed radius for the Galaxy.
In 1922 Edwin Hubble described the relative dimensions of M31 and the Galaxy as follows Hubble (1929): "A tentative comparison of sizes, masses luminosities, and densities suggests that the *galactic system is much larger than M31* but that the ratio is not greater than that between M31 and other known extra-galactic systems." More recent estimates for this distance range from 700 to 810 kpc (see table 1).

[1]From the centre of the Milky Way

Article	orientation
Dubinski et al. (1996)	(240,-30)
Gott and Thuan (1978)	(242,-30)
Metz et al. (2007)	37.7, 77.5
Koch and Grebel (2006)	37.7±0.2, -12.5
Gott and Thuan (1978)	52±2,77±3

Table 2: Orientation of the spin axis of Andromeda. Dubinski et al. (1996) and Gott and Thuan (1978) are in galactic coordinates. Metz et al. (2007) Koch and Grebel (2006) and Gott and Thuan (1978)(measured clockwise from east) use equatorial coordinates (PA and inclination). Cox and Loeb (2007) do not mention their used orientation.

Article	Position
Binney and Tremaine (1987)	(121.2, -21.6)
Sparke and Gallager (2000)	(121, -22)
Dubinski et al. (1996)	(121, -23)
Evans and Wilkinson (2000)	(121.2, -21.6)
Gott and Thuan (1978)	(121, -22)
Metz et al. (2007)	(121.7, -21.5)

Table 3: Position

2.4.2 Orientation Spin Axis

In table 2 we give an overview of several articles and the different orientations they use for the Spin axis of Andromeda.

2.4.3 Distance and Position

The values provided in tables 3 and 1 can be combined to give the exact position of Andromeda.

2.4.4 Extent / Radius

Visible Galaxy
The radius is a difficult parameter to describe. The edge of a galaxy is not so well defined. One possibility is to look at the optical disk radius. You can also define the radius of the disk to be where the density drops to a certain part of the central density.

Dark Halo
Even more difficult to define is the radius/extent of the dark halo. For convenience we adopt the Milky Way radius from Kuijken and Dubinski. In table 4 we have two articles that have defined a radius for both Andromeda

Article	R_d M31 (kpc)	R_d MW (kpc)
Dubinski et al. (1996)	5.8 ± 0.3	4.5 ± 1
Kuijken and Dubinski (1995)	-	4.5
Cox and Loeb (2007)	3.6	2.2

Table 4: Disc scale radi of Andromeda and the Milky Way (kpc)

Article	Radial Velocity(km/s)
Binney and Tremaine (1987)	-119
Dubinski et al. (1996)	-130
Sparke and Gallager (2000)	-299
Gott and Thuan (1978)	-93
Evans and Wilkinson (2000)	-123
Cox and Loeb (2007)	-120
Loeb et al. (2005)	-117

Table 5: Galactocentric Radial Velocity Andromeda, Sparke and Gallager (2000) use heliocentric velocity with the velocity of the Sun towards the Galactic centre -10 km/s.

as the Milky Way. They find ratios of $R_{M31}/R_{MW} = 1.3$ (Dubinski et al., 1996) and $R_{M31}/R_{MW} = 1.6$ (Cox and Loeb, 2007). We assume a ratio of 1 for R_{M31}/R_{MW}.

Intergroup medium

How empty is space in between Andromeda and the Milky Way? Cox and Loeb (2007) claim there is an intra group medium, which consists of dark matter and gas. This medium causes dynamical friction, which shortens the time of first passage.

Article	Transverse/tangential Velocity(km/s)
(Dubinski et al., 1996)	26 or 20
(Evans and Wilkinson, 2000)	0
(Cox and Loeb, 2007)	< 200
(Loeb et al., 2005)	100 ± 20
(van der Marel and Guhathakurta, 2007)	42

Table 6: Transverse Velocity Andromeda

2.4.5 Begin Velocities

The radial velocity of Andromeda is well known (Table 5 [2]), but this is not the case for the transverse velocity. The radial velocity can be derived by redshift measurements. For Andromeda we adopt a radial velocity of -117 km/s. This is in galactocentric coordinates $\mathbf{v}_{\mathrm{M31}} = (56.4; -91.87; 45.48)$ km/s. But Andromeda is to far away to see the transverse velocity with an optical telescope. Since the best optical telescopes can detect motions of 0.2 milli-arcseconds per year (Brunthaler et al., 2007b), with simple geometry this sets the limit to Andromeda's maximum transverse velocity of 700 kilometers per second (heliocentric).
With the observed velocities of more nearby galaxies, and assuming them bound to Andromeda, more precise estimation can be made. Loeb et al. (2005) used the measured proper velocity of M33 and the timing argument to constrain the proper motion and total mass of Andromeda (without 'intermediate' dark matter distribution in the local group, neglection of previous interactions and assuming constant mass for the systems for the past 10 Gyear). They use $M_{\mathrm{M31}} = 3.4\ 10^{12}$ and $M_{MW} = 2.3\ 10^{12}$. Based on numerical simulations they find a transverse velocity of 100 plus min 20 [3]. They find that the dark halos of Andromeda and the Milky Way will pass through each other within the next 5 to 10 Gyr.

Recent studies show that water masers can give an exact measurement as well. Brunthaler et al. (2007b) measure the proper motion of a water maser in Galaxy IC 10 (distance ∼660 kpc) relative to two background quasars. With this velocity and under the assumptions that IC10 is bound to Andromeda and that IC10 and Andromeda have not had a close encounter in the past, they deduce a lower limit on M31's mass of $7.5\ 10^{11} M_{\odot}$.

In a recent paper van der Marel and Guhathakurta (2007) use several indirect measurements of the transverse velocity and combine them to find a weighted average transverse velocity of 42 km/s, with 1σ confidence interval $V_t = 56$ km/s. More about this in the discussion.

Absolute used values for the transverse velocity vary from zero to two hundred kilometers per second (see table 6). The main goal of this research is to check what the effect of the transverse velocity is on (the possibility of) the merger.

We want to find a lower limit for the transverse speed for which there will be no collision between Andromeda and the Milky Way. To achieve this

[2] The rotation velocity is also well known, but difficult to compare since literature gives the rotation velocity as a function of the radius. Therefor we will just adopt the rotational velocity used in Kuijken and Dubinski.

[3] With quadrant of a negative velocity component along right ascension and a positive component along declination strongly ruled out

we approximate both galaxies by pointmasses. We assume the galaxies are bound. A recent paper by (Niemi et al., 2007) shows that based on the comparison of numerical simulations to observations of kinematics for the nearby (< 40 Mpc) groups of galaxies, 80 percent of these groups are bound. The Milky Way and Andromeda are bound if:

$$E = 0.5\mu|\mathbf{V}_{\rm rel}|^2 - \frac{G\mu M}{|\mathbf{r}_{\rm rel}|} < 0. \tag{1}$$

Where M is the total mass, μ is the reduced mass:

$$\mu = \frac{M_{\rm M31} M_{\rm MW}}{M}, \tag{2}$$

$\mathbf{V}_{\rm rel}$ and $\mathbf{r}_{\rm rel}$ represent the relative velocity and location vector of the Andromeda with respect to the Milky Way and G is the gravitational constant.

So the 'point mass' galaxies are bound if

$$M > \frac{|\mathbf{r}_{\rm rel}||\mathbf{V}_{\rm rel}|^2}{2G}. \tag{3}$$

And if the $\mathbf{V}_{\rm rel} = \sqrt{\frac{2GM}{|\mathbf{r}_{\rm rel}|}}$, this gives a unbound (parabolic) orbit, where the galaxy velocities equal the escape velocity at each point of the orbit. We fill in (galactocentric coordinates, kpc):

$$\mathbf{r}_{\rm M31} = (-378.3; 615.4; -304.8), \tag{4}$$

$$\mathbf{r}_{\rm MW} = (0; 0; 0), \tag{5}$$

$$\mathbf{r}_{\rm rel} = \mathbf{r}_{\rm M31} = (-378.3; 615.4; -304.8), \tag{6}$$

$$\tag{7}$$

and for the relative velocity $\mathbf{V}_{rel}$ we use the radial velocity. This way we find a minimum value for the total mass of both galaxies, corresponding with the case the galaxies started out with zero velocity, so they follow a radial orbit (directly towards each other) and have zero angular momentum. The minimal total mass we find with equation [3] is$10^{12} M_\odot$. We use

$$\mathbf{r}_{\rm CM} = \frac{M_{\rm M31}\mathbf{r}_{\rm M31} + M_{\rm MW}\mathbf{r}_{\rm MW}}{M}, \tag{8}$$

$$\mathbf{V}_{\rm CM} = \frac{M_{\rm M31}\mathbf{v}_{\rm M31} + M_{\rm MW}\mathbf{v}_{\rm MW}}{M}, \tag{9}$$

and change our velocity and position vectors to centre of mass coordinates.

Article	**Mass M31** ($\times 10^{11}$ $M_\odot$)	**Mass MW** ($\times 10^{11}$ $M_\odot$)
Dubinski et al. (1996)1	11-36	5-17
Evans and Wilkinson (2000)	12.3^{+18}_{-6}	19^{+36}_{-17}
Brunthaler et al. (2007a)	7.5	-
Gott and Thuan (1978)	11.5	11.5
Loeb et al. (2005)	34	23
Widrow et al. (2003)A	4.15-12.7	
Cox and Loeb (2007)	16	10
Kuijken and Dubinski (1995)	-	3.17-19.5

Table 7: Mass Andromeda and Milky Way.

2.4.6 Mass

The mass calculated using visible light of the disk and the mass calculated using kinematics, differ a lot.
The total mass according to Table 7 for Andromeda varies between 4 and 36×10^{11} $M_\odot$ and for the Milky Way between 3 and 55×10^{11} $M_\odot$. Recent studies by (Brunthaler et al., 2007a) use the velocities of IC 10 and M33 and by comparing this to the escape velocity for the case IC10 and M33 are bound to M31, they deduce a lower limit for the mass of Andromeda of 7.5 10^{11} $M_\odot$. This is a factor of 2.4 larger than the mass for Andromeda that is favoured in the paper by Widrow et al. (2003). Originally we wanted to use Widrow's mass because his findings, based on observational data for the rotation curve, inner velocity dispersion profile and surface brightness profile, are very convincing (see Appendix C for some discussion).

We note (see table 7) that there is a wide variety of estimates. This is not strange since the halo extent, that determines the total halo mass and the total galaxy mass, is not very well known. So we must keep in mind that there is a large errorbar on both the individual masses as on the mass ratio of the two galaxies. Most people believe Andromeda to be the more massive of the two, but Evans and Wilkinson (2000) argue that the Galaxy is the biggest. Also Gott and Thuan (1978) find Andromeda and the Galaxy to be approximately of the same mass, though they also mention a massratio of M_{MW}=1.25M_{M31}. van der Marel and Guhathakurta (2007) assume mass ratios of $M_{\rm M31}/M_{\rm MW}$=0.8-2.0

Based on the luminosity ($L_{\rm M31} = 2L_{\rm MW}$), disk scale length ($R_{d_{\rm M31}}$ about $2R_{d_{\rm MW}}$), rotation (Rotation M31 about 1.2-1.3 $\times$ Rotation MW) and the number of globular clusters ($N_{glob_{\rm M31}} > 2N_{glob_{\rm MW}}$) Sparke and Gallager (2000) argue Andromeda is the larger of the two galaxies. Kuijken and Dubinski (1995) use in their models a total Milky Way mass ranging from $\sim 3 - 20 \times 10^{11}$ $M_\odot$. Because there is no definite answer about correct mass

ratio, we will use the same masses for both galaxies. We decided to use K&D models, so in order to exceed the minimal mass we found in the previouw section, we will use model D. This model has masses of $1.95 \times 10^{12} M_{\odot}$ so they total $3.9 \times 10^{12} M_{\odot}$. With equation [3] this leads to a maximum absolute (relative) velocity of 207 km/s which gives a maximum transverse velocity of 171 km/s, assuming a bound orbit.

Binney and Tremaine (1987) derive a formula where with the current measured velocity and separation and an estimate of the age of the universe, a mass estimate for the two galaxies can be made. This model is known as the *timing argument* and it is based on the assumption that M31 and the MW were formed on very close distance almost immediately after the big bang, and have masses high enough to overcome the cosmic expansion.
Orbits with a velocity lower then the maximum relative velocity lead to a bound, elliptical orbit. With $v_{\rm rel}$= 207 km/s, $M_{\rm t}$ = 3.9 $10^{12} M_{\odot}$ and a separation of 784 kpc, and without making any strong assumptions about on what part of the orbit we are, we calculate the semi major axis a of the system to be

$$a = 1/\left(\frac{2}{r_{\rm rel}} - \frac{(v_{\rm rel})^2}{M_t} G\right) \sim 10^6 kpc. \tag{10}$$

With as a minimum velocity the already observed radial velocity of 117 km/s, we find a semi major axis of ∼575 kpc. With the semi major axis we can also calculate the period

$$P = \frac{2\pi}{\sqrt{G M_{\rm MW} M_{\rm M31}}}\, a^{\frac{3}{2}} \tag{11}$$

to be $\approx 5.2\ 10^{13}$ year for the largest axis and $\approx 2\ 10^{10}$ year for the minimal period. Since we assume the galaxies are approaching for the first time, we know the age of the universe has to be between 0.25 and 0.5 times the period. This gives us, for the lowest velocity, ages between $5\ 10^9$ and 10^{10} years. And for the highest velocity, ages between 1.3 and 2.6 times 10^{13} years. With the current estimates of the universe age of about 13.8 Gyr, we can rule out the higher values for the semi major axis and thus for the higher transverse velocities. For the lower estimated value we find a semi major axis shorter than the separation we currently observe, so the lowest value of v_{rel}=117 km/s can also be ruled out, so $v_t \neq 0$.

2.4.7 First approach vs. transverse velocity

As the time of first approach we use the moment of closest approach of the centers of mass of both galaxies. To estimate this time we calculate the time

it would take for two point particles to fall towards each other, on a purely radial orbit when nothing except gravity acts on them.

$$\ddot{\mathbf{r}} = \frac{-GM_{\text{tot}}}{\mathbf{r}^2}, \tag{12}$$

$$\int \ddot{\mathbf{r}}\ \dot{\mathbf{r}}\ dt = -\int \frac{GM_{\text{tot}}}{\mathbf{r}^2}\ \dot{\mathbf{r}}\ dt, \tag{13}$$

$$\frac{\dot{\mathbf{r}}^2}{2} = \frac{GM_{\text{tot}}}{\mathbf{r}} + C, \tag{14}$$

$$|\mathbf{v}_0| = \sqrt{\frac{2GM_{tot}}{R} + 2C}, \tag{15}$$

$$C = \frac{{\mathbf{v}_0}^2}{2} - \frac{GM}{R}, \tag{16}$$

$$\frac{dr}{dt} = \sqrt{\frac{2GM_{\text{tot}}}{\mathbf{r}} + {\mathbf{v}_0}^2 - \frac{2GM_{\text{tot}}}{R}}, \tag{17}$$

$$\frac{dt}{dr} = \frac{1}{\sqrt{\frac{2GM_{\text{tot}}}{\mathbf{r}} + {\mathbf{v}_0}^2 - \frac{2GM_{\text{tot}}}{R}}}, \tag{18}$$

$$\int_0^{t_{end}} dt = \int_R^0 \frac{1}{\sqrt{\frac{B}{\mathbf{r}} + A}}\ dr \tag{19}$$

Where $A = {\mathbf{v}_0}^2 - \frac{2GM_{\text{tot}}}{R}$ and $B = 2GM_{tot}$. With the above calculation we can plot the estimated time of first approach as a function of mass (figure 8), initial velocity (figure 9) and initial separation (figure 7).

Of course we must remember that we made the assumption that we deal with point particles, but this seems to be a good approximation since initially the galaxies are far from each other.

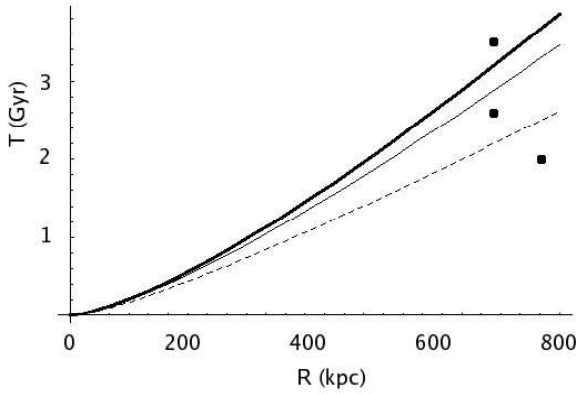

Figure 7: Calculated time of first approach versus initial separation for three different radial velocities: 90 (heavy line), 117 (line) and 200 km/s (dashed line), mass=3.9 $10^{12} M_{\odot}$. Dots represent measured values according to (from top) Dubinski et al. (1996) low mass model, high mass model and Cox and Loeb (2007).

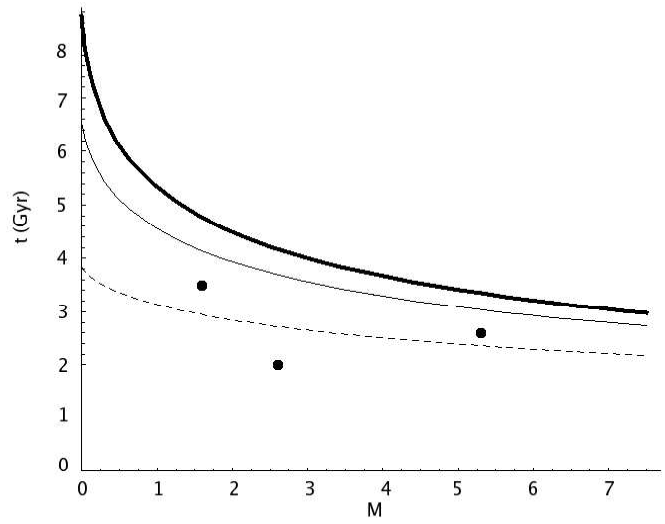

Figure 8: Calculated time of first approach versus mass for three different radial velocities: 90 (heavy line), 117 (line) and 200 km/s (dashed line). Dots represent measured values according to (from left) Dubinski et al. (1996) low mass model, high mass model and Cox and Loeb (2007).

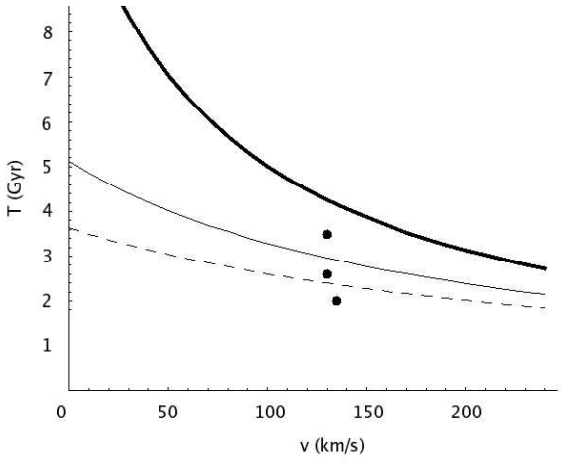

Figure 9: Calculated time of first approach versus initial (absolute) radial velocity for three different masses: 1 $10^{11} M_{\odot}$ (heavy line), 5 $10^{11} M_{\odot}$ (line) and 1 $10^{12} M_{\odot}$(dashed line). Dots represent measured values according to (from top) Dubinski et al. (1996) low mass model, high mass model and Cox and Loeb (2007).

3 Methods

To get an idea about what will happen during a possible merger between Andromeda and the Galaxy, we will perform N-body simulations. In this chapter we describe some necessary steps for setting up such a simulation. We will also compare three different computer algorithms and test what is the best code to use.

3.1 N-body modelling

In this section we give a short overview of N-body simulations in general.

Force
For N-body systems the only force acting on a particle i, is the gravitational force:

$$\mathbf{F}_i = \sum_{j \neq i} G \frac{m_i m_j (\mathbf{r}_i - \mathbf{r}_j)}{|\mathbf{r}_i - \mathbf{r}_j|^3}. \tag{20}$$

Together with $\mathbf{F}_i = \frac{m_i \partial^2 \mathbf{r}_i}{\partial t^2}$, these functions determine the equations of motion. These equations of motions can be solved numerically if N=2, but lead to a problem when N≥3. For more than 3 particles the integrals can only be solved by numerical integration (except for some special cases). This means that the integral is approximated by the evaluation of the integrand, using sufficiently small steps. The size of this timesteps depends on the nature of the system, on the error that is acceptable, and on the numerical integrator you use.

Another problem with equation [20] is that for small separation the denominator goes to zero. This leads to problems which can be solved by setting a smoothing length ϵ:

$$\mathbf{F}_i = \sum_{j \neq i} G \frac{m_i m_j (\mathbf{r}_i - \mathbf{r}_j)}{(|\mathbf{r}_i - \mathbf{r}_j|^+ \epsilon^2)(3/2)}. \tag{21}$$

ϵ is typically chosen $1/N$.

3.2 Time scales

For N-body simulations to be as simple and efficient as possible, you want to get rid of as many unnecessary factors as possible. This is why in N-body modelling it is standard to use N-body units, where the total mass, the gravitational constant and energy are as follows:

$$G = M = -4E = 1 \tag{22}$$

With the use of standard N-body units, the velocity dispersion equals $1/\sqrt{2}$ and the crossing time equals $2\sqrt{2}\times$ natural unit of time, the fiducial time [4]. The relaxation time is the time it takes for particles to have so much interaction that it perturbes the system. Our used K&D-models (Kuijken and Dubinski, 1995) have a unit mass of 5.1 10^{10} $M_{\odot}$, a unit length of R_d = 4.5 kpc, and a unit velocity of v=220 km/s. With G=1, this corresponds to a natural unit of time of $t = 20\ 10^6$ year.

Number of particles/ resolution

One problem with the creation of a N-body galaxy system is the formation of a stable disk. When two bodies come very close their gravitational pull exceeds the 'smooth' force they feel from all particles in the system. For stars in a galaxy however, this number of close encounters is very small. Therefore the individual stars follow orbits that are described by the smooth potential of the total system. Disk galaxies are not relaxed systems, e.g. they do not change much over time because of collisions. These collisions perturb the velocities in the system, they allow particles to exchange energy and momentum, and thereby make these velocities random. Also the collisions cause mass segregation: heavier bodies tend to end up more centrally distributed and lighter bodies in the outer regions. These collision effects are also known as *two body relaxation*. To prevent the possibility of particle collisions that make the disk unstable, you need a smooth potential. A smooth potential means a 'homogeneous' distribution of particles. To accomplish this, the mass of the halo particles can not be to high compared to the disk and bulge particle masses. The disk remains stable if the halo particles are maximum ten times the mass of the disk and bulge particles (at least for the K&D-models). We will test this in the following section.

Scaling

A star cluster generally contains between 10^4 to 10^6 stars. This is the approximate limit for the direct method. Since typical galaxies contain about 10^{11} stars, these systems can not be calculated using the direct method.

3.3 Algorithms

In this subsection we describe two calculation methods to calculate the force.

Direct methods

If you want to have the lowest possible errors in your simulation, you should use a direct method. The direct method calculates all the forces between the individual particles: this comes down to $\frac{1}{2}N(N-1)$ calculations for N particles. Twice as much particles lead to about 4 times as many calculations, the computation time scales with $O(N^2)$. It is clear that for simulations with high particle numbers, the direct method is not preferred. But of course the

[4] ref: http://en.wikipedia.org/wiki/Natural_units

choice of calculation depends on the nature of the system.

Treecodes
Barnes and Hut (1986) presented their tree code method that by a smart approximation, minimizes the total number of calculations. Instead of calculating all forces between all particles, first they divide space in equal boxes and divide these boxes in equal sized daughter boxes again (since we have a 3D space this comes down to a division by 8). They keep dividing the parent box until all particles in the system have a private box. Second they construct the tree, leaving out empty boxes, and they do this reconstruction for each time step. Now instead of calculating all these forces for each particle, this is approached by replacing a group of particles with a pseudo particle, located at the centre of mass of the group. The average size of the created boxes that contain a particle is comparable to the spaces between particles. With l the length of the box, and D the distance from the box's centre of mass to the particle you calculate the force on, they created the accuracy parameter θ (also known as the opening angle). The process of dividing boxes in smaller boxes continues until $l/D < \theta$. The higher the value for the opening angle, the earlier the tree is build (smaller height of the tree), but this also gives a larger error. The computation time of these tree codes scales as $O(N \log N)$. For collisionless systems the treecode has a good performance.

GPU
The realisation that computational improvement only could increase as fast as the increasing technology, triggered the developement of special purpose hardware (Portegies Zwart et al., 2007). Meanwhile a similar process was (and still is) going on in the gaming industry: demands about the graphical representations kept growing, and better and better graphics cards were developed. These cards are very good at fast calculations; when you watch something that happens fast, you want the computer to be able to represent this. To do this each changing (colour of the) pixel has to be calculated very rapidly. Fortunately this can be done parallel, because one pixel does not require information about the other pixels. This fast calculation property makes the GPU very suitable for doing simulations that require lots of 'simple' calculations, exactly what is needed in N-body simulations. The GPU has a theoretical peak performance of about 500 GFLOP/s (500 billion floating-point operations per second) which is about 50 times faster than a regular computer. In practice the GPU is about twenty times faster than the normal computer.

η n_{crit}	2	3	4
16384	x		
32768	x	x	x
65536	x	x	x
131072	x	x	x

Table 8: Used n_{crit} and η

3.4 Choice of code

We use tree treecodes for the simulations. On the PC we use *hackcode1* (an equal-timestep implementation of a hierarchical N-body code (Barnes and Hut, 1986)) and *gyrfalcON* (with individual adaptive time steps and individual (but fixed) softening lengths (Dehnen, 2000)). We also use *nbody-g6*, which is a treecode initially created to run on a Grape (Makino, 2004) but now adjusted for use on the GPU (Belleman et al., 2008) , with some alterations by Harfst (2008)[5]). To check whether the GPU is a good device for these simulations, we perform two test: we check the t_{CPU} as a function of particle number (for integration time $t_{int} = 10$) and we compare the energy error of the three codes. For all three codes we use opening angle $\theta = 1$ and softening parameter $\epsilon = 0.05$. For both nbody-g6 and gyrfalcON we use timestep dt=1/64 (64 timesteps per integration timestep), for hackcode1 we use a timestep of dt=1/32. For other input parameters for hackcode1 and gyrfalcON we use the default values. For nbody-g6 we also set the parameter n_{crit}, the critical Barnes vectorization parameter. This parameter determines whether a 'treecodebox' should be split into daughterboxes or not. We set $n_{crit} = 32768$, so if $N > 32768$ particles the boxes will be split. We also set the critical value for the force calculation (in file kirin.cfg) to 16384 (Belleman et al., 2008).

Figure 10 shows that hackcode1 has not our preference, because it is already 4 to 7 times slower than the other two codes and it already has a longer time step (so it does less calculations per integration time). Based on this graph it would be best to use gyrfalON for 88000 particles.

We also look at the energy error ($dE = |\frac{E_0 - E(t)}{E_0}|$) as a function of running time for the three codes, see figure 11. We notice that, based on the energy error, again hackcode1 is the least favourable (but we must keep in mind that the energy error decreases with number of timesteps per integration time, so this graph does not give a fair representation of dE for hackcode1 since we used a twice as long timestep. The simulations we run on the GPU and with gyrfalcON are comparable.

Based on the t_{CPU} and dE, we can conclude that nbody-g6 and gyrfalcON are both suitable codes to use for our experiment. We choose the GPU

[5]Quote Harfst: 'The code hasn't changed, I just changed the way it is programmed.'

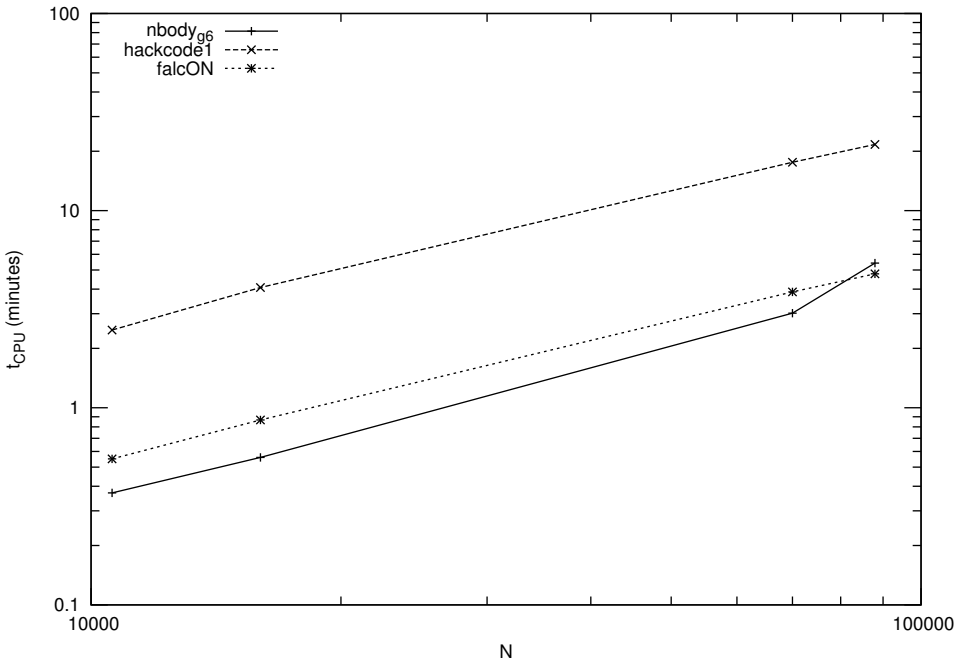

Figure 10: CPU time versus number of particles for integration time $t_{int} = 10$ for the three different codes, nbody-g6 (solid line), hackcode1 (dashed line) and falcON (dotted line).

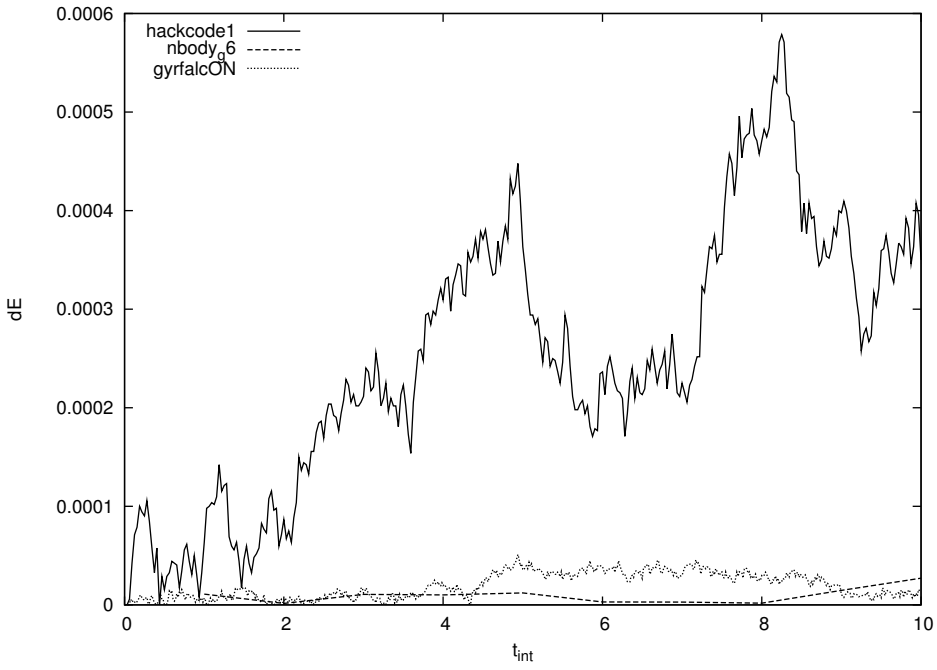

Figure 11: Energy error as a function of integration time, for the three different codes, hackcode1 (solid line), nbody-g6 (dashed line) and falcON (dotted line).

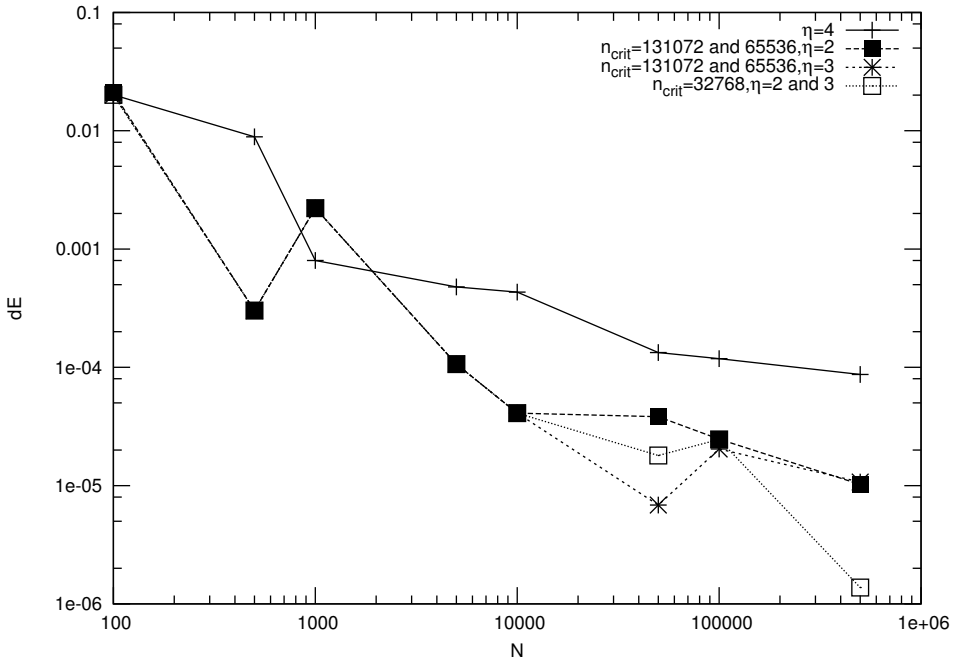

Figure 12: Energy error as a function of N for different values of n_{crit} and η. For η=4 we find the dE vs N dependence, not to depend on values of n_{crit} (crossed upper line). For η=2 and n_{crit}=128 k or 64 k we find the dE vs N dependence represented by the filled squares. For η=3 and n_{crit}=128 k or 64 k the dE vs N dependence is represented by stars. For n_{crit}=32 k and values of η of 2 and 3 the results are represented by the open squares.

because it offers an interesting new way for doing simulations.

To choose the best initial parameters for our simulations, we have created 8 models with different particle numbers in the range of 100 to 500,000 particles. We run these with the GPU for $t_{int} = 1$. The number of timesteps that is used depend on the value of η. This parameter partially determines the number of timesteps that are taken within one integration time. The size of the time step depends on η, the softening ϵ, the particle velocity v_i and accelaration a_i. The size of the timestep equals η times the minimum of ϵ/v_i or $\sqrt{\frac{\epsilon}{a_i}}$. We use values for η and n_{crit} as described in table 8, for all models with different N. Then we look at the t_{CPU} and the energy error dE.

Based on figure 12 we conclude that the lowest energy errors occur for N>50,000, where the curve flattens. Since using a higher particle number does not seem to affect the decrease of energy error that much anymore, we decide that our choice of 88000 particles is a legitimate one. We also notice that for the higher timestep η=4, the error on average is about ten times higher than for smaller values of η. This is why we decide not to use these

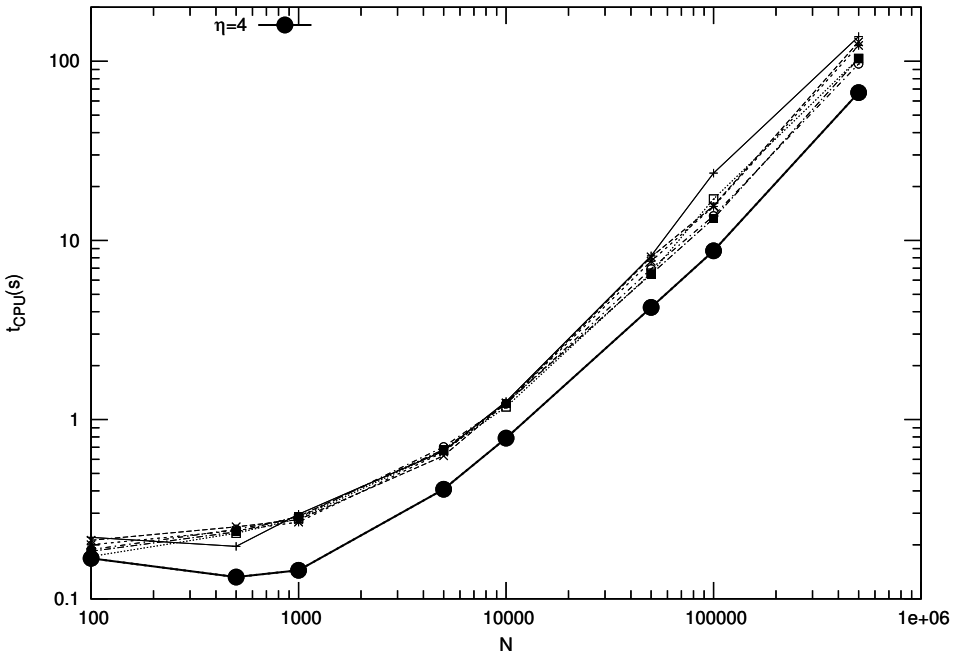

Figure 13: t_{CPU} as a function of N for different values of n_{crit} and η. For η=4 we find the t_{CPU} vs N dependence not to depend on a different value of n_{crit} (thick line with heavy dots). All other combinations of values for n_{crit} and η lead to comparable t_{CPU} vs N dependence (represented by all other lines).

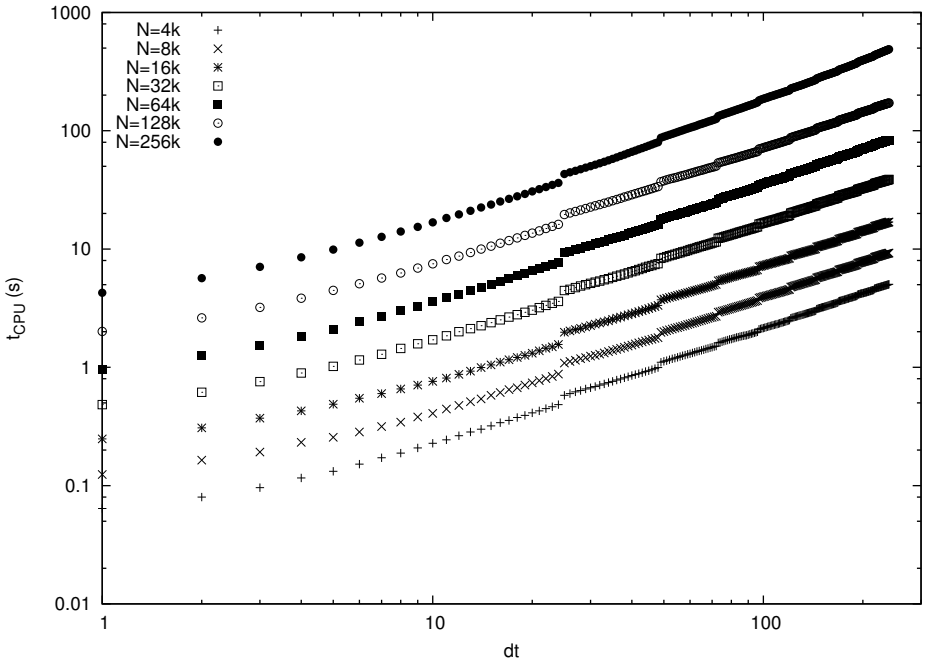

Figure 14: t_{CPU} as a function of dt, with n_{crit}=32768 and nkirin=32768.

large timesteps. The figure also shows that for N=500,000, it is best to use $n_{crit} = 32768$.

Figure 13 shows that for η=4 the t_{CPU} is at least almost a factor of two faster than with the other timesteps, but we already decided not to use this, based on the energy error. The curved shape of the graph, for low values of N, can be explained by overhead; it takes some time to start up. We also notice that for more than 5000 particles the lines are more or less straight. This means that the computer is optimally used.
We conclude that for our 88000 particle system we use $\eta = 3$ and $n_{crit} = 65536$.

To examine the effect of the number of particles on the GPU, we used different particle numbers (ranging from N= 4 k to N=256 k) for our simulations, and check how the CPUtime evolves as a function of N (we use ncrit and nkirin= 32 k). We use a timestep dt=1/24, and in figure 14 we can see that output is writed out every 24 timesteps, which cost time. Figure 15 shows that for particle numbers lower than 16 k, the t_{CPU} increases with N. For higher particle numbers the CPUtime starts to behave more like $N \log N$ (very roughly), and for even higher particle numbers, it looks like the CPUtime increases with N^2.

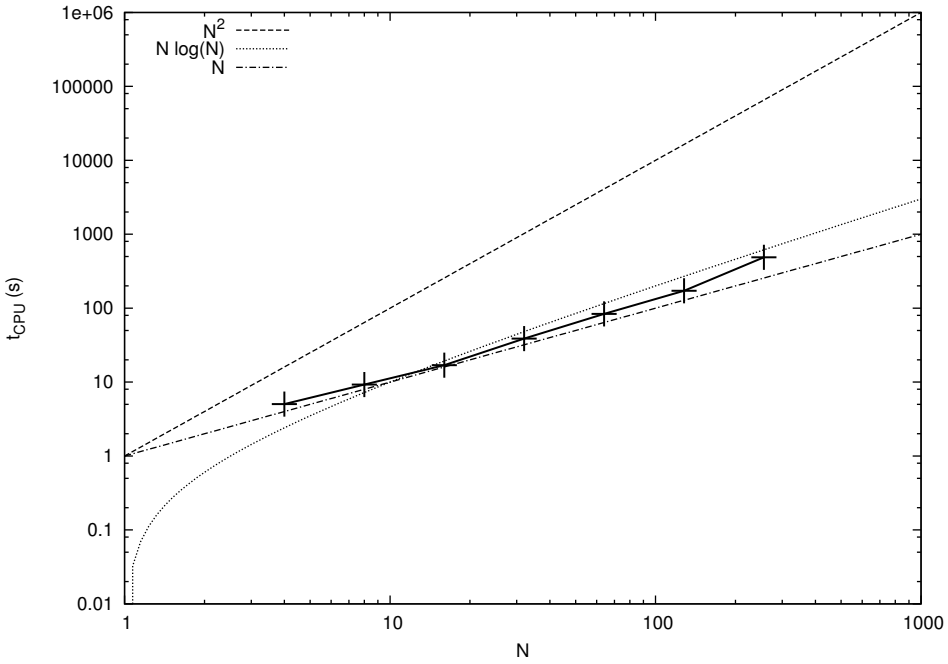

Figure 15: t_{CPU} as a function of the number of particles, with n_{crit}=32768 and nkirin=32768.

We also examine the effect of particle number on the physics of the system. We look at the separation between the galaxies as a function of time, for particle numbers between 11000 and 176000. We notice that for particle numbers of 44000 and higher, the lines converge. This can also be seen in figure 17. So with 88000 particles we have picked the right number of particles.

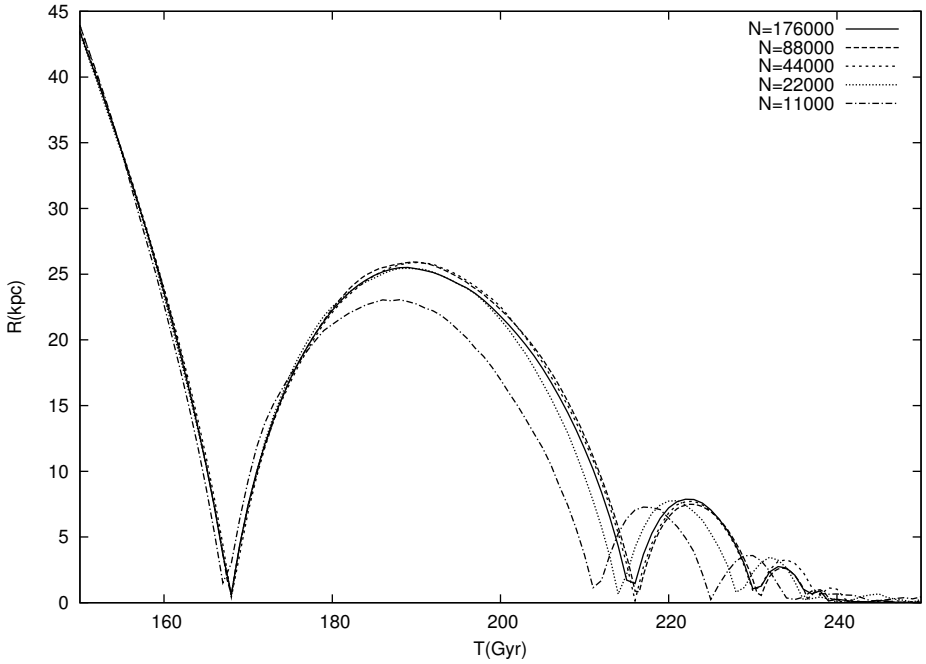

Figure 16: The separation between M31 and the MW, for different N.

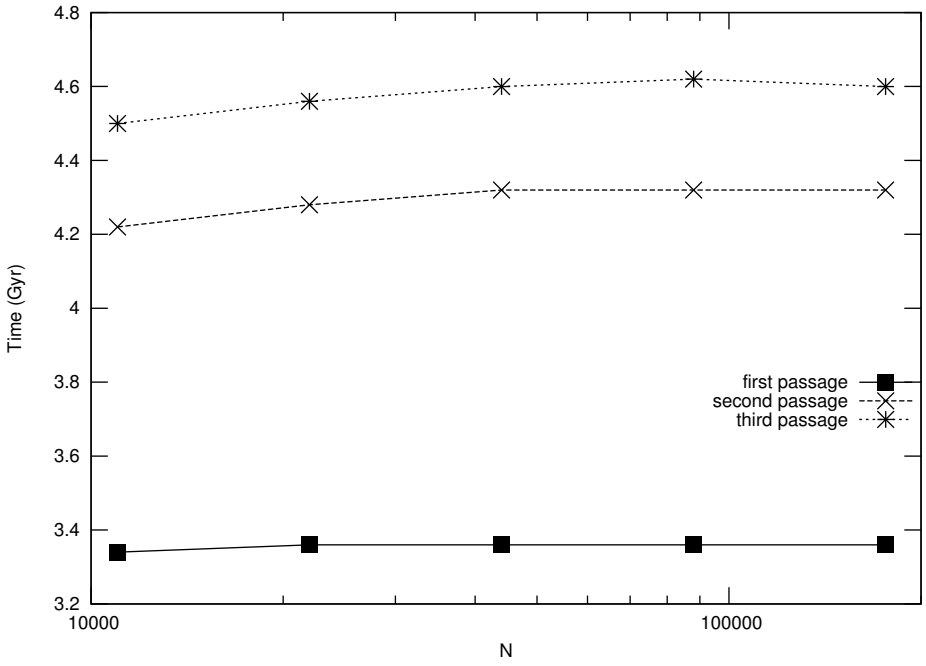

Figure 17: Time of first, second an third approach as a function of N.

4 Set up galaxies

For our galaxies we use NEMO, the program galactICS, created by Kuijken and Dubinski (1995). In the first subsection we will give a short overview of their model set up. In the second paragraph some more about our initial conditions.

4.1 Creating K&D-galaxies

We have decided to use Kuijken and Dubinski (K&D) models to create the Milky Way and Andromeda. Kuijken and Dubinski (1995) created a set of models that all represent the observed rotation curve of the Milky Way, but have different halo extents, and therefore different halo masses. In this section we give an overview of the different distribution functions for the bulge, halo and disk, and a summary of our used parameters.

The potential that describes an N-body system with a lot of particles can be modeled under the assumption that there is a smoothed out density structure. It is not smart to add the different potentials of all individual bodies, since typical values for the number of stars in a galaxy are 10^{11}. Anton Pannekoek already spoke of *statistical astronomy* (Murdin, 2001):

"It appears where we have to deal not with stars individually but, with hundreds or thousands of even millions of them. Then the nature of the problem has changed with the object; we do not ask which stars, but how many stars have certain characteristics (color, spectrum, duplicity) or certain values of the parameters (temperature, density luminosity, magnitude). Counting supplies the measuring. The positions (in the sky of in space) do not matter, but the densities of distribution (over the sky or over space). Statistical laws of distribution are the objects and the working instruments of the astronomer who is dealing with thousands and millions of the heavenly host."

Setting up an N-body simulations starts with choosing a distribution function. Such a function defines a set of initial positions and velocities for particles with a known mass. The choise of potential determines, with the use of the Poission equation, the density profile (the initial distribution of particles). With known initial velocities, positions and masses, and provided that the only interaction is by gravity, we can use equation [20] to find the equations of motion.

Distribution functions and density profile
For the bulge distribution function (DF) K&D use a King model (King, 1966). This model represents a spherically symmetric system, so the distri-

bution function follows from the functions for energy and angular momentum per unit mass. The distribution function (f_b) a of the bulge is as follows:

$$f_b(E) = \begin{cases} \rho_b(2\pi\sigma_b^2)e^{\Psi_0-\Phi_c/\sigma_b^2}(e^{-(E-\Phi_c)/\sigma_b^2}-1) & \text{if } E < \Phi_c, \\ 0 & \text{otherwise.} \end{cases} \quad (23)$$

The bulge DF depends on the cut-off potential of the bulge (Φ_c), the bulge central density (ρ_b) and the velocity dispersion (σ_b).

For the halo distribution function (f_h) K&D use a lowered Evans model. These are models that, like the King model, depend on the integrals of motion of energy and angular momentum, that follow a logarithmic flattened potential.

$$f_{halo}(E, L_z) = \begin{cases} [(AL_z^2 + B)e^{-E/\sigma_0^2} + C][e^{-E/\sigma_0^2} - 1] & \text{if } E < 0, \\ 0 & \text{otherwise.} \end{cases} \quad (24)$$

So the halo DF depends on the velocity scale σ_0 and the energy which is defined by the depth of the potential well (σ_0). A, B and C are defined by the flattening parameter (q), the halo core radius (R_c) and a characteristic halo radius (R_a).

For the distribution function of the disk a third integral of motion is needed to describe the vertical energy component, because the velocity dispersion in radial and vertical direction differ. The disk is described by the following parameters: mass (M_d), radial scale length (R_d), scale height (z_d), disk truncation radius ($R_o uter$) and the truncation width (δR_{trunc}). For a good description of the disk distribution function we advice to read the original article 'Nearly self-consistent disc-bulge-halo models for galaxies' by Kuijken and Dubinski (1995).

To find the combined potential K&D first calculate the density profiles by integrating the individual DF's over all velocities. To make sure that the final model created with the three DF's is self gravitating, the combined potential needs to be implied by the Poisson equation.

Summary of input parameters

For a summary of the used input parameters we refer to Appendix A, table 10. Some important properties of the models are not direct input parameters, for instance M_b, M_h and the tidal radius of the halo can not be chosen directly. If you want to change the halo mass, but keep the values for the bulge and disk reasonably constant, this can be done by changing the central potential, central velocity and cut off potential.
Because of reasons described in the chapter 2.4 and appendix C, we have decided to use model D of the K&D-models.

Used particle numbers We have checked what would be the best ratio of disk+bulge vs halo particles (see previous section) by using a constant

number of disk (Nd) and bulge (Nb) particles and varying the number of halo particles (Nh). We used Nd=8000, Nb=2000 and Nhalo=600, 6000 and 60000. The resulting disks at three different moments are shown in figure 18. As expected it appears that for more halo particles the disk is more stable. This is also proven by the effect that the total energy, figure 19, does a better job remaining constant for higher particle numbers, and the energy error decreases with increasing particle numbers, figure 20.

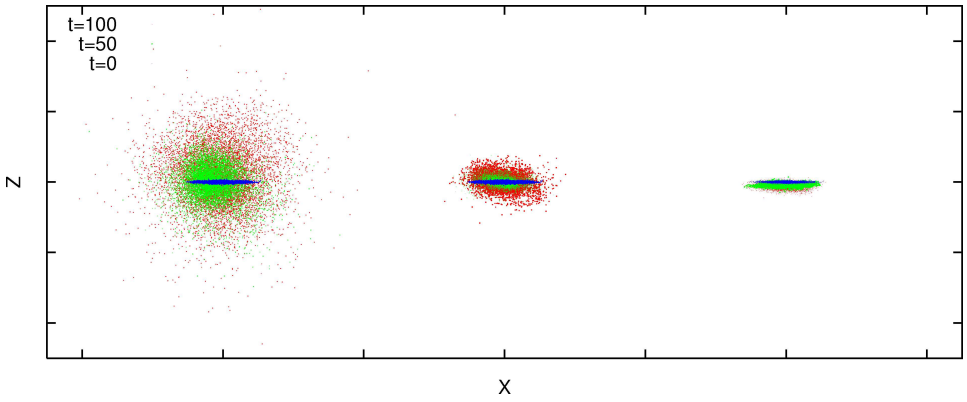

Figure 18: Galaxy disk thicknesses at three different moments: t=0 (blue), t=50 (green) and t=100 (red), with Nd=8000, Nb=2000 and (from left to right) Nh=600, 6000 and 60000.

Based on these figures we decide to use 2000 bulge particles with mass 11 $10^6 M_\odot$ and 8000 disk particles with mass 5.6 $10^6 M_\odot$. Since the halo particles can not be more than ten times as massive as the lightest particles, we must use 34000 halo particles, with mass 56 $10^6 M_\odot$.

4.2 Set up merger model

4.2.1 Orientation

According to Dubinski et al. (1996) Andromeda's spin axis in galactic coordinates points to the direction $(l, b) = (240, -30)$ when the rotation axis of the Milky Way points at $(0, -90)$. Galactic or Heliocentric Coordinates (see Appendix B) take the Sun as its centre, and are a right handed coordinate system with the positive x-axis pointing to the centre of the Galaxy. To give Andromeda the right position and rotation, we first rotate the right-handed coordinate system counterclockwise around the z-axis with 240° :

$$Q_{\mathbf{z}}(\theta) = \begin{pmatrix} \cos\theta & -\sin\theta & 0 \\ \sin\theta & \cos\theta & 0 \\ 0 & 0 & 1 \end{pmatrix} \tag{25}$$

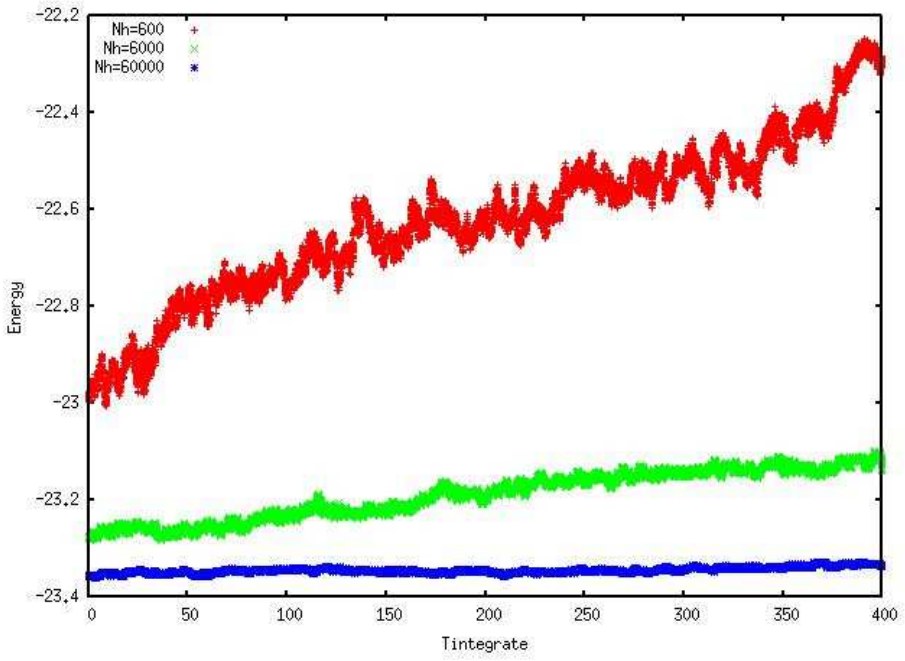

Figure 19: Energy as a function of integration time, with Nd=8000 and Nb=2000 and Nh=600, 6000 and 60000.

Now we want to rotate around a unit-vector **u** (the new y-axis), that has the coordinates (0.866, -0.5, 0).

$$Q_{\mathbf{u}}(\theta) = \begin{pmatrix} 0 & -z & y \\ z & 0 & -x \\ -y & x & 0 \end{pmatrix} \sin\theta + (I - \mathbf{u}\mathbf{u}^T)\cos\theta + \mathbf{u}\mathbf{u}^T \quad (26)$$

$$= \begin{pmatrix} (1-x^2)\cos\theta + x^2 & -z\sin\theta - xy\cos\theta + xy & y\sin\theta - xz\cos\theta + xz \\ z\sin\theta - xy\cos\theta + xy & (1-y^2)\cos\theta + y^2 & -x\sin\theta - yz\cos\theta + yz \\ -y\sin\theta - xz\cos\theta + xz & x\sin\theta - yz\cos\theta + yz & (1-z^2)\cos\theta + z^2 \end{pmatrix} \quad (27)$$

Now we do a rotation of $\theta = -60°$, then our matrix looks like:

$$\begin{pmatrix} 0.875 & -0.2165 & 0.433 \\ -0.2165 & 0.625 & 0.75 \\ -0.433 & -0.75 & 0.5 \end{pmatrix} \quad (28)$$

We use the above matrix both for the coordinate transformation and the velocity component transformation.
There still is a small difference between the rotation according to (Metz et al., 2007) and (Dubinski et al., 1996). Metz et al. did not use galactic

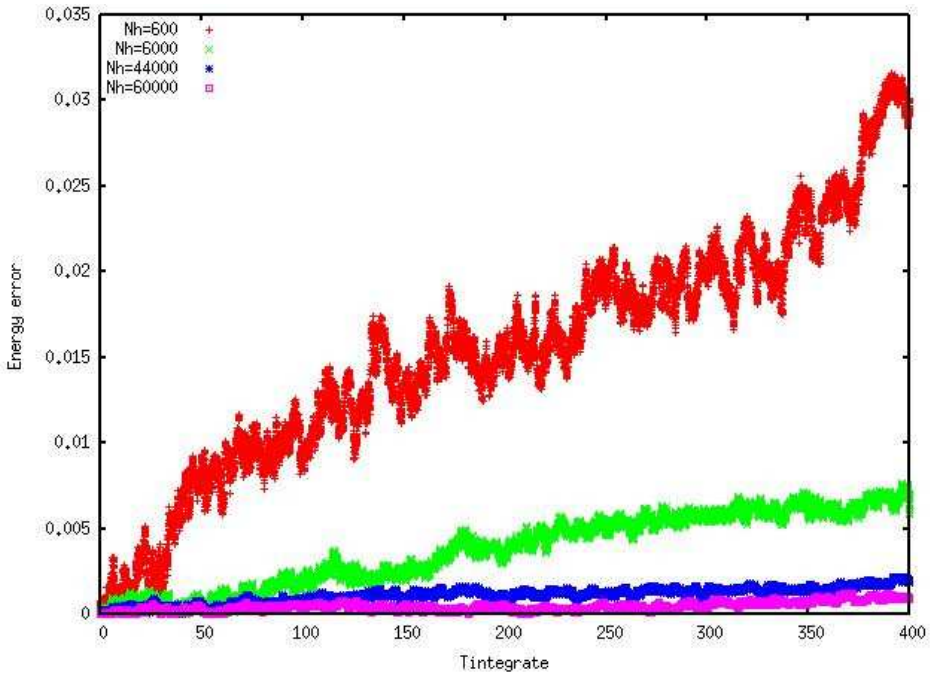

Figure 20: Energy error as a function of integration time, with Nd=8000 and Nb=2000 and Nh=600, 6000, 34000 and 60000.

coordinates for the rotation axis to orient Andromeda, instead they used equatorial coordinates. We agree with them that the rotation by Koch and Grebel (2006) cannot be right.

4.2.2 Distance, position and velocities

After we give Andromeda the right rotation coordinates, it is time to put Andromeda at the correct location. To achieve this we use again galactic coordinates. According to (Dubinski et al., 1996) Andromeda is positioned at **(l,b)=(121,-23)**. We transform these coordinates to Cartesian coordinates by applying the following:

$$x = D\cos b\cos l \tag{29}$$

$$y = D\cos b\sin l \tag{30}$$

$$z = D\sin b \tag{31}$$

D stands for the distance from the Sun to Andromeda.

We have decided to use the estimated distance of **780 kpc**[6]. We find

[6]We also use the extreme estimates to find out the earliest/latest time of approaching.

that Andromeda is positioned at $\mathbf{r} = (-369.8, 615.4, -304.8)kpc$ (Cartesian coordinates, figure 33). This is comparable with (van der Marel and Guhathakurta, 2007), they find a position of (-379.2, 612.7, -283.1)[7] If we take the distance of the Sun to the Galactic centre to be 8.5 kpc, we find the galactocentric coordinates for Andromeda: $\mathbf{r} = (-378.3, 615.4, -304.8)kpc$ this leads to a distance between the centres of $784kpc$.

To position Andromeda and the Milky Way at the correct location, we simply add the x-,y- and z-values, corrected for the centre of mass, to the original positioning vector[8]. We also do this for the velocities.
To create a transverse velocity component, e.g. a vector perpendicular to the radial component, we do the following: We choose $v_1 = v_r$ and v_2=(1,0,0), a vector in the plane of the galaxy (not rearranged for the centre of mass yet). Then we take the orthogonal projection of v_1 on v_2, by taking the inner product of v_1 and v_2, divide that by the innerproduct of v_1 and multiply by the vector v_1 . Next we substract this projection from v_2, which gives us v_t. To check whether the vectors v_r and v_t really are perpendicular we normalize both and take the inner product, which equals zero, so that is good.

[7]They adopt a distance of 770 kpc and use a galactocentric coordinate system, with a distance of the Sun to the Galactic Centre of 8.5 kpc.

[8]We use K&D's natural units for length, velocity and mass.

5 Results

In this chapter we describe our main results concerning the collision possibility, the structure after the collision and the future location of the Sun.

5.1 Collision probability

To examine the effect of the magnitude of the transverse velocity, we have added a velocity component to the original velocities. We used six different transverse velocities, with a maximum of 171 km/s, corresponding to the highest possible transverse velocity where the (point mass) galaxies are still bound. We run the simulation as described in subsection 3.4.
The resulting separation between Andromeda and the Milky Way as a function of time, is plotted in figure 21. We notice that on a purely radial orbit, the time of first aproach is about 3.4 Billion years. This is approximately the same result as what we calculated assuming the galaxies to be point masses (see figures 22 and 24). Figure 22 also shows that with a relatively low mass, Cox and Loeb (2007) manage to have a very fast time of approach. This is because of the intragroup medium (of dark matter and gas) they use. This medium causes dynamical friction; it extracts orbital energy and angular momentum which speeds up the merger process. When looking at this plot, one sees that even though we have an about 2.5 times higher mass than the lower mass model of Dubinski et al. (1996), their time of approach is comparable. This can be explained by the difference in initial separation of the two simulation setups.

To determine a measure for the collision 'stage' of the system, we plot the moments of closest encounter as a function of transverse velocity, figure 25 and we plot the distance of close encounters as a function of transverse velocity, figure 26. By extrapolating the time of second approach, $t_{\rm sa}$, versus transverse velocity, we find a function that depends on ${v_t}^4$.
Figure 27 shows the total energy as a function of time, calculated using equation 1 under the assumption that the galaxies are pointmasses, located at the centre of density of the individual galaxies. We notice that all galaxy pairs with $v_t < 171$km/s are indeed bound. The orbit with a transverse velocity of 171 km/s has a constant energy, the galaxies have hardly any interaction. This can also be seen in figure 28. Since the orbits with transverse velocities lower than 171 km/s are bound, we can use the above found relation to estimate a time of second approach for the orbits with $86 < v_t < 171$. For a v_t of 107 km/s we find a $t_{\rm sa}$ of about 15 Gyr, 129 km/s leads to $t_{\rm sa} \sim$ 27 Gyr.
The radius of our halos is about 330 kpc, so for all used values of v_t the halos have some interaction (see figure 26). This does not seem to affect the disks much. The disks only start to change in morphology when they really touch. In chapter 6 we will have some discussion about how realistic this is.

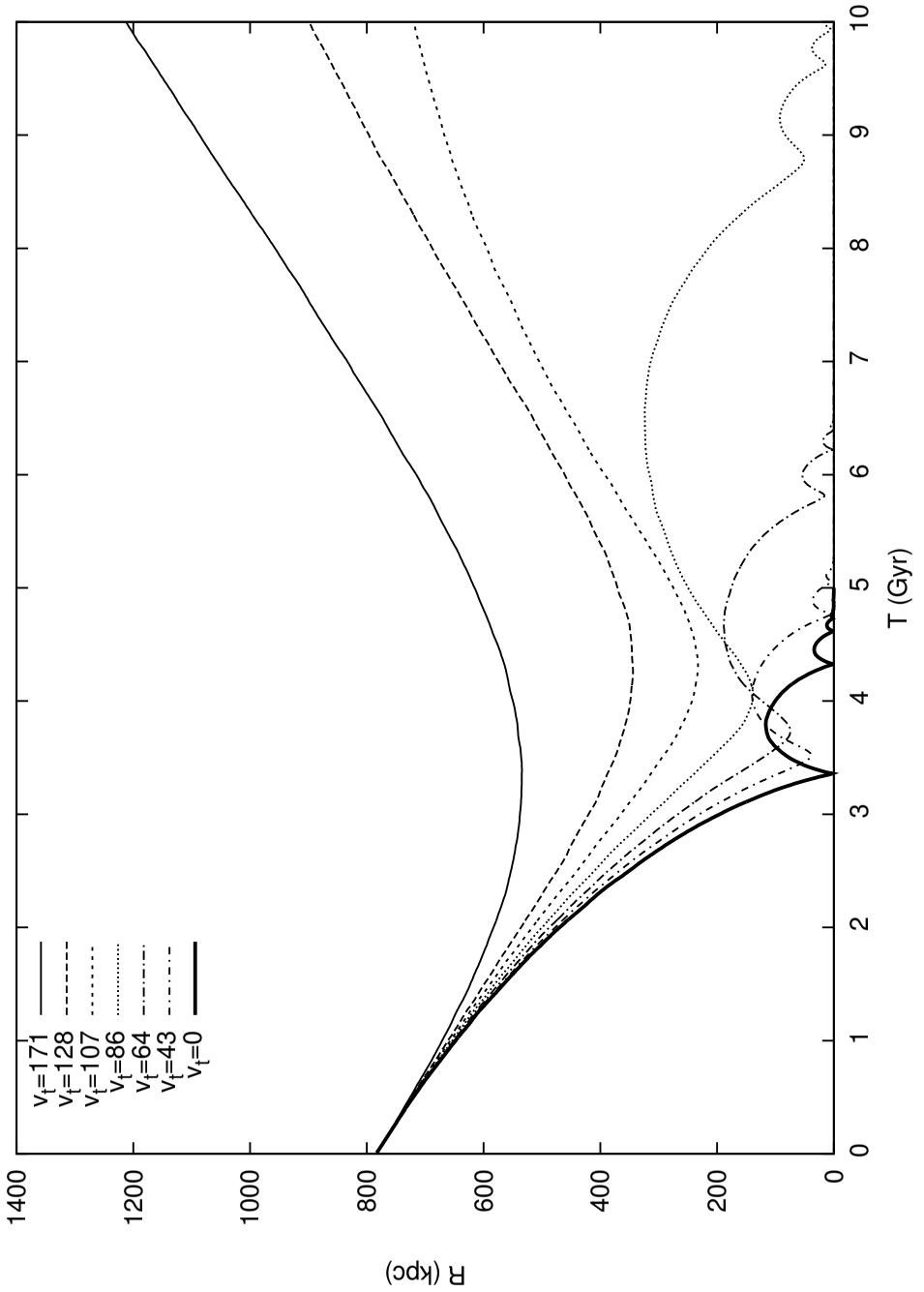

Figure 21: The separation between M31 and the MW, for transverse velocities up to 171 km/s.

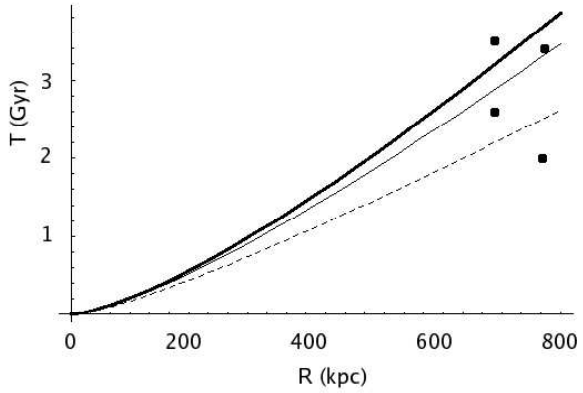

Figure 22: Calculated time of first approach versus initial separation for three different radial velocities: 90 (heavy line), 117 (line) and 200 km/s (dashed line), mass=3.9 $10^{12} M_{\odot}$. Dots represent measured values according to (from top) Dubinski et al. (1996) low mass model, our result, Dubinski et al. (1996) high mass model and Cox and Loeb (2007).

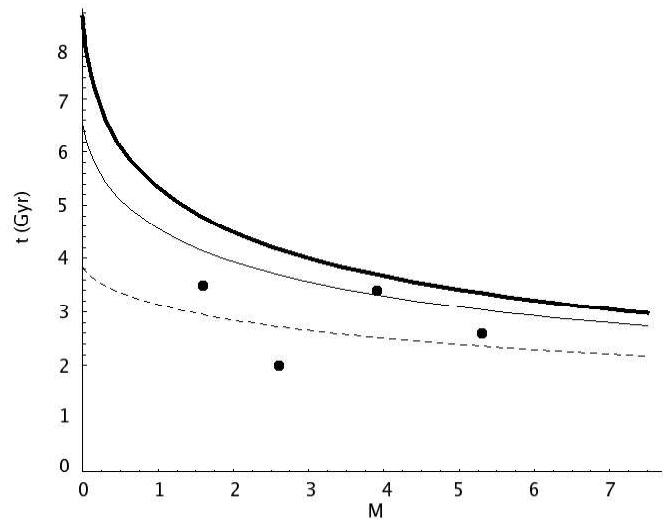

Figure 23: Calculated time of first approach versus mass ($\times 10^{12} M_{\odot}$) for three different radial velocities: 90 (heavy line), 117 (line) and 200 km/s (dashed line). Dots represent measured values according to (from left) Dubinski et al. (1996) low mass model, Cox and Loeb (2007), our result and Dubinski et al. (1996) high mass model.

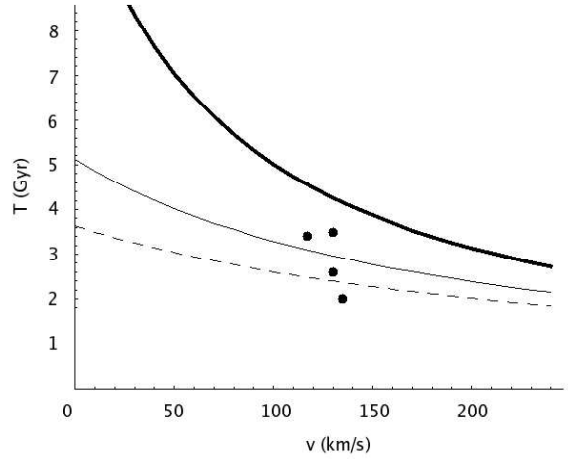

Figure 24: Calculated time of first approach versus initial (absolute) radial velocity for three different masses: $10^{11} M_{\odot}$ (heavy line), 5 $10^{11} M_{\odot}$ (line) and $10^{12} M_{\odot}$ (dashed line). Dots represent measured values according to (from top) Dubinski et al. (1996) low mass model, our results, Dubinski et al. (1996) high mass model and Cox and Loeb (2007).

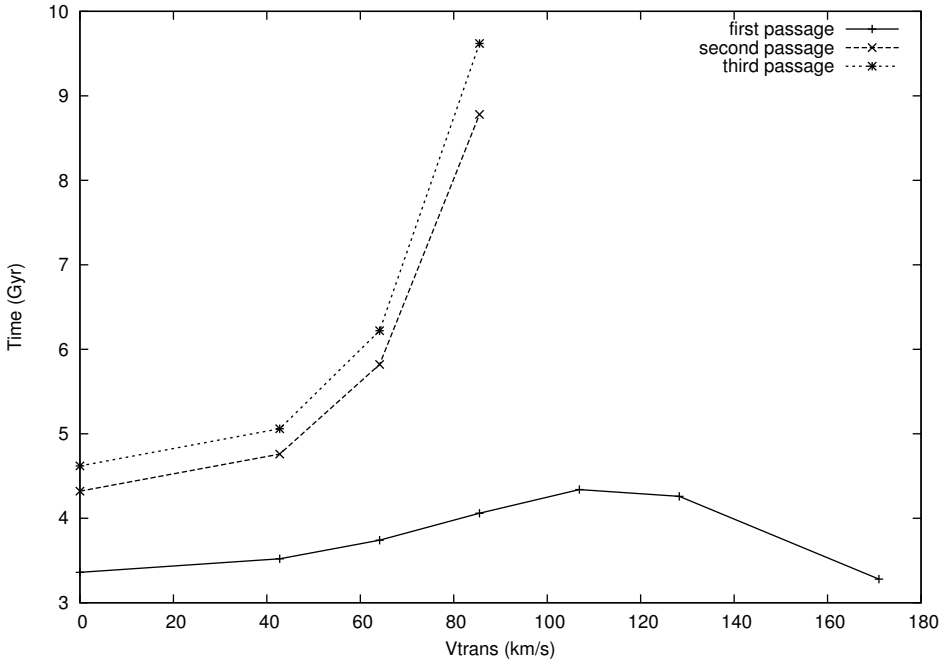

Figure 25: Approach time (Gyr) versus initial transverse velocity (km/s).

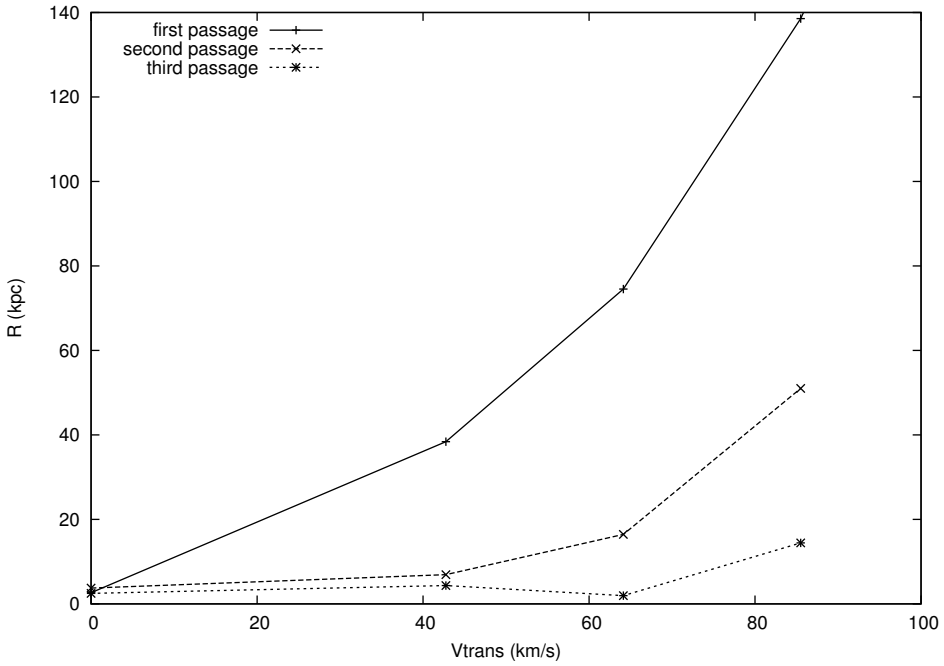

Figure 26: Separation (kpc) at closest passage versus initial transverse velocity (km/s).

5.2 Structure after collision

Looking at figures 29 and 30, we notice that collisions with an initial transverse velocity of 86 km/s or higher will not lead to the formation of one galaxy within 10 Gyr, simply because they do not have a second, close enough passage within this timescale. Lower velocities do lead to the formation of an elliptical galaxy.
Comparing the images of our simulation to the Toomre sequence (see figure 4) is not very easy. Our galaxies do not show tidal features as strong as the ones in the Toomre sequence. This can be seen in Figure 29, the Milkomeda during collision does not form really long tidal tails. This agrees with the article by Dubinski et al. (1996). They found that collisions of galaxies with massive halos do not form real tidal tails. Massive mergers have higher potential wells. This has two effects: their encounter velocity is higher, this detunes the resonance between orbital angular frequency and the internal angular frequency of the disk stars (which is needed to produce tidal tails) and the escape velocity of the stars is higher, so less stars can escape to form tidal tails. Figure 30 shows the Milkomeda after 10 Gyr[9]. These images do not only show that for the higher initial transverse velocities there will be

[9]Paul Melis and Robert Belleman created a movie of the data for v_t=64 km/s. This movie can be seen on http://staff.science.uva.nl/ paul/overview.avi

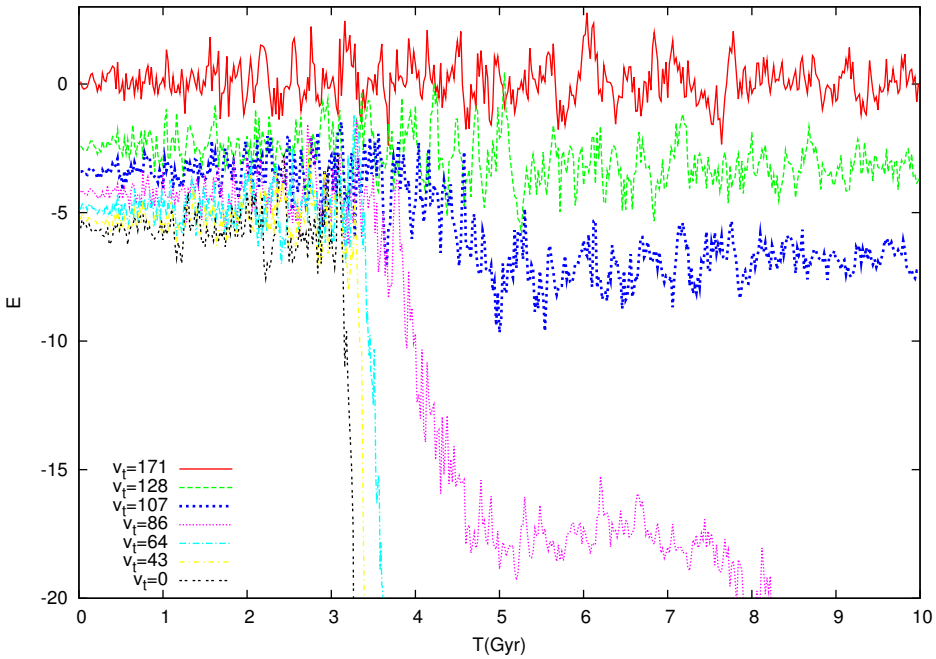

Figure 27: Total energy in K&D units as a function of time (Gyr), for different initial values of the transverse velocity: v_t=171 km/s (red), 128 (green), 107 (blue), 86 (pink), 64 (light blue), 43 (yellow) and v_t=0 (black).

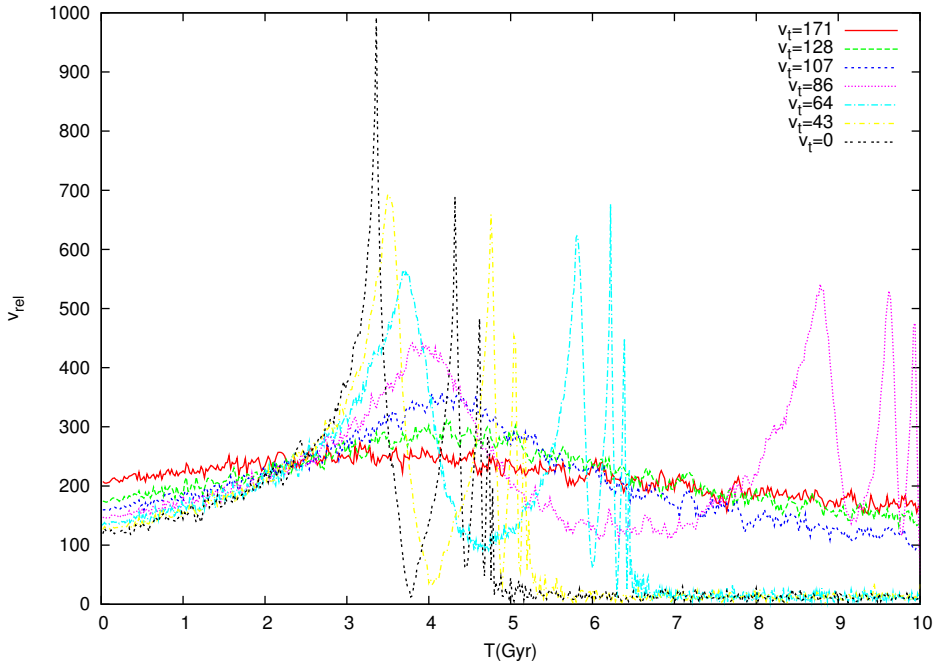

Figure 28: Relative velocity of the two galaxies as a function of time (Gyr), for different initial values of the transverse velocity : v_t=171 km/s (red), 128 (green), 107 (blue), 86 (pink), 64 (light blue), 43 (yellow) and v_t=0 (black).

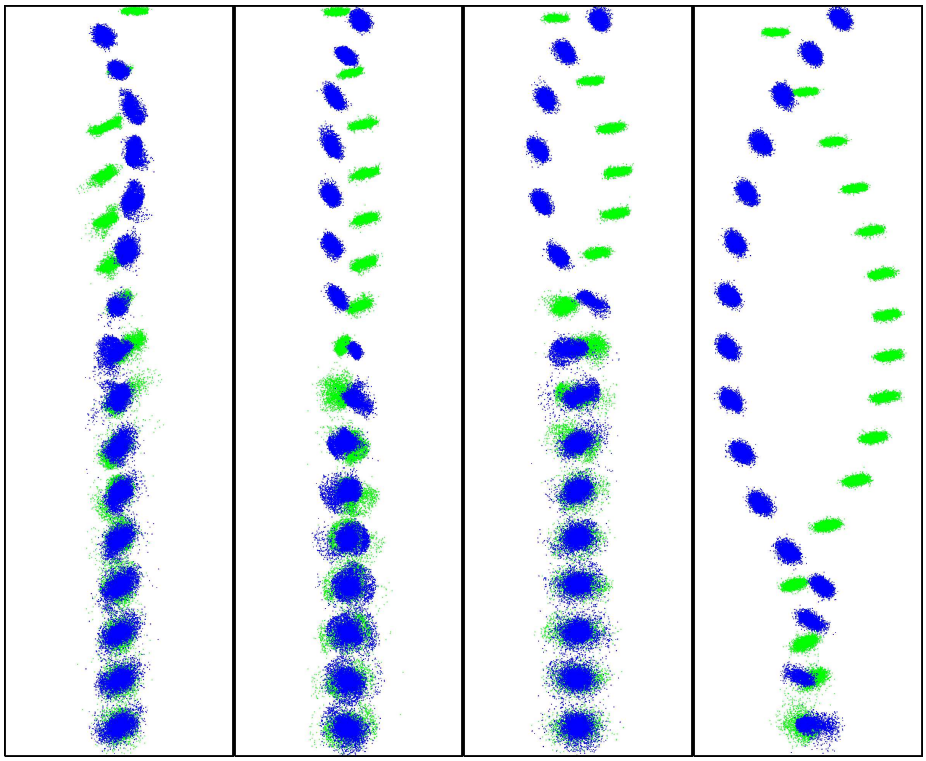

Figure 29: Collisions with v_t=0, 43, 64 and 86 km/s, viewed from the y-direction, width of the image equals 450 kpc. The first strip (from left) starts at t=3.16 Gyr, then steps of 0.2 Gyr. Second strip starts at t=3.44 Gyr, then steps of 0.2 Gyr. Third strip starts at t=3.64, then steps of 0.4 Gyr. The last strip starts at t=4 Gyr, then steps of 0.4 Gyr.

no definite merger within 10 Gyrs, they also show that the eventual shape of Milkomeda depends on the transverse velocity. The mergers with initial velocities of 43 and 64 km/s have a spherical distribution, but the merger with zero v_t has a more elongated structure. The reason for this is probably that with zero transverse velocity the angle at which the galaxies hit differs from the angle at higher transverse velocities. This can also be seen in figure 29.

5.3 Location of the Sun

To investigate the effect of the merger on the location of the sun, we followed solarlike (radius 8± 0.1 kpc) particles in time. (Cox and Loeb, 2007) also did this and they found that the possibility existed that during the merging process the sun would get gravitationally bound to Andromeda before the two galaxies collide. As is seen in figure 31 we do not observe any solarlike particle (pink in figure) to get bound to Andromeda. This does not mean

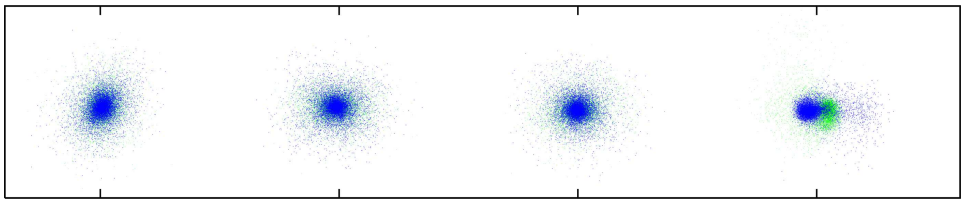

Figure 30: Milkomeda at t=10 Gyr, for (from left) v_t=0, 43, 64 and 86 km/s.

there is something wrong with the paper by Cox and Loeb (2007), they only find 2.7% of the solarlike particles to behave in this manner. Since we only found 98 solarlike particles in our sample (8000 disk particles), it is not unlikely we do not detect these particles (Cox and Loeb (2007) use 14350 disk particles in their simulation). Another difference we discover when comparing our galaxies during the merger process with theirs, is that their merger does form tidal tails. This can be explained by the fact that they use gas and an intermediate dark matter distribution ànd have a lower total mass for the galaxies. The two results can not be compared because the initial conditions differ too much.
Since the Sun's luminosity and size will increase due to hydrogen burning, this will affect the atmosphere and therefore life on Earth. (Kasting, 1988) calculated that in about 1.1 Gyr the luminosity will be about 10% higher, which causes the atmosphere's water molecules to evaporate. In about 3.5 Gyr the increase of brightness will be about 40 - 50 %, which means the sea's also are evaporated. Life on earth will become impossible. Since our calculated earliest time of approach between the two galaxies is in 3.4 Gyr, it is safe to say that no human (descendant) will observe this from earth.

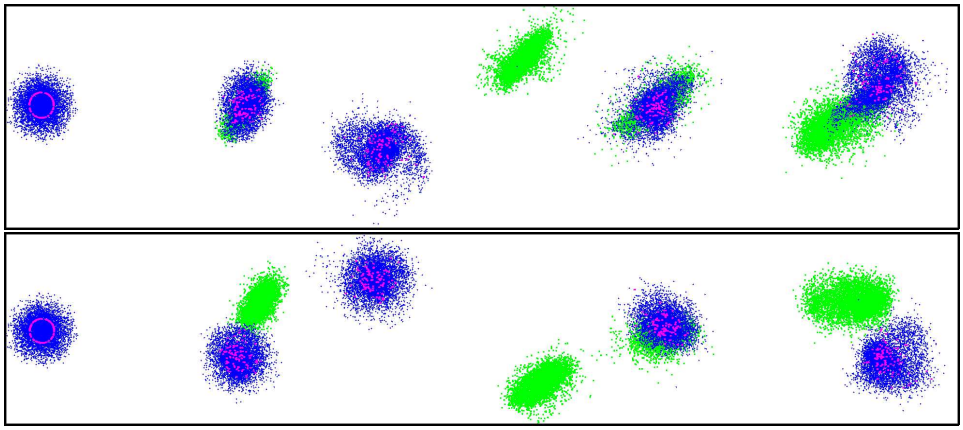

Figure 31: Merger between Milky Way (blue) and Andromeda (green) with selected solar like particles (pink), observed from xy-plane (perpendicular to MW disk). Top strip has v_t=0 km/s, first image (from left) is today, then the first passage (t=3.36 Gyr), then post-first passage (t=3.84), second passage (t=4.32) and post-second passage (t=4.48). Bottom image has v_t=43 km/s, first image from left is today, then first passage (t=3.52), then post-first passage (t=4.14), second passage (t=4.76) and post-second passage (t=4.92).

6 Discussion and Recommendations

To evaluate this research we have chopped the discussion in three parts; first we will have a discussion concerning our main question: will Andromeda and the Milky Way collide? Second we will discuss the limitations on our research and do some propositions for future research, and third we will have a short discussion concerning the work process.

6.1 Milkomeda?

During this research a lot of things we assumed to be known, turned out to be uncertain. Like, are groups of galaxies (and more specific - is the local group) bound or not? What is the combined mass of Andromeda and the Milky Way, and what is their mass ratio? And what is the transverse velocity of Andromeda with respect to our galaxy?
Of course these questions depend for a big part on the same question: what is the nature of dark matter and how is it distributed in space? Without making any assumptions it is impossible to give a definite answer to our main question. We can only say something genuine about the collision probability with our used parameters. With our used conditions the answer is that it is very likely that there will be a collision. The most recent estimate for the transverse velocity favours a value of about 42 km/s (van der Marel and Guhathakurta, 2007). With this velocity the first approach will be in 3.5 Gyr and the Milkomeda will be fully merged in 5.5 to 6 Gyr. Though the research presented by van der Marel and Guhathakurta (2007) seems very thorough, it is based on a lot of assumptions. Four different methods find various values for the transverse velocity. Weighting their average is a reasonable thing to do.
The article of van der Marel and Guhathakurta (2007) is very recent, not yet refereed and in fact still a draft version. Double checking their results is of crucial importance for our conclusions. If we discard their results, and base our conclusions on other estimates (e.g. by Loeb et al. (2005) that used the undisturbed M33 disk found velocities of about 100 km/s), our derived chance that Andromeda and the Galaxy will not merge within the next 30 Gyrs will increase significantly, and then there is even the possibility that the galaxies will not merge at all.

6.2 Future research

Limitations
This section deals with the main limitations of this research.

We did not change the parameter 'nkirin' for running the simulations on the GPU with program nbody-g6. We expect that changing this parameter

to a number comparable with n_{crit}, can possibly improve the performance.

We only measured the stability of the disk to a timescale of about 2 Gyr, the time we initially expected the first collisions to occur (based on the simulations with intragroup medium by Cox and Loeb (2007)). To make the disks stable over longer timescales, we probably should use higher numbers of particles. We do not expect the instability of the disk has had a great effect on time of first approach of the galaxies, but it can have an effect on the morphology (and kinematics) of the merger remnant.

We used two similar galaxies to represent Andromeda and the Milky Way. Though we do not assume a slightly different mass ratio, disk radius or rotation velocity will change the time of approach much, these parameters can greatly effect the merger remnant. We already observe that only changing the transverse velocity component can have a significant effect on the shape of the merger.

Though in galaxies gas is important for star formation and causes extra friction, in our model we did not include gas. Cox and Loeb (2007) did use gas in their model. They compared the star formation as a function of time for Andromeda and the Milky Way as isolated galaxies and as merging galaxies, and found no significant difference. They explain this by the fact that at this moment there already is little gas in the systems, but that at the time of the merger ($\sim$ 2 Gyr in their simulation) most (>75%) of this gas will be used for star formation. Since our merger timescale is even longer, we conclude that using gas particles will not improve the results, since hardly any gas will be present at collision time.

The galaxy models provided by Kuijken and Dubinski (1995) are good to use for our purpose: studying the effect of the transverse velocity on the timescale of merging. But for an even more realistic model we would recommend to use the models by Widrow and Dubinski (2005). These include a central black hole. The great advantage of these models over the K&D-models, is that important properties of the galaxy can be directly chosen as input parameters.

In our calculations we only use the masses of Andromeda and the Galaxy. Of course there is other mass in the local group, that interferes with the models. But since M31 and the MW make up about 80% of the luminous matter (Sparke and Gallager, 2000), we think this is a good assumption. Even better would be to add M33, which contains 10% of the visible matter.

Recommendations
Based on the above discussion we recommend the following improvements

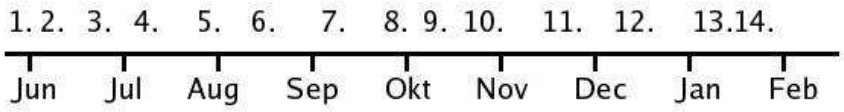

Figure 32: Timeline of work process, for explanation numbers see text.

for this research:

- Use more particles for the simulations, to create stable galaxies over longer periods.
- Double check the results of van der Marel and Guhathakurta (2007), to give more definite estimates on total mass and transverse velocity.
- Use several different halo masses.
- Use of a M31:MW mass ratio and rotation velocity $\neq 1$, which agrees better with current observations.
- Use the galaxy building algorithm provided by Widrow and Dubinski (2005).
- Add M33 to the simulations.

6.3 Concerning work process

In this paragraph we will give a short time line with the most important steps of this research, figure 32. We shortly discuss the steps that did not go so well, that for instance took too much time.

1. Choose a project. Simon Portegies Zwart had the GPU ready for use and was looking for interesting Nbody simulations to test this. After some discussion and reading (Cox and Loeb, 2007) we decide to do a simulation of the collision of Andromeda and the Milky Way and compare this with their results
2. Read articles about the subject and keep track of new articles
3. Find a paper Kuijken and Dubinski (1995) and decide to use their code to run the simulations and compare our work with their results
4. Choose the program NEMO for the creation of my initial galaxies and figure out how to use the program
5. Search for initial conditions
6. Read more about galaxy evolution
7. Find out that v_t is not known very well

8. Several articles, e.g. (van der Marel and Guhathakurta, 2007) claim that the masses should be higher, we decide not to change our initial conditions because paper by Widrow et al. (2003) is convincing

9. Decide to use v_t as main research parameter

10. Decide that the used masses are to low

11. Run simulations with different values for vtrans

12. Find out that multiplying the halo mass with 10 is not allowed and that the paper by Widrow et al. (2003) is not reproducable

13. Use GPU and check the gyrfalcON code as well

14. Decide that hackcode1 is not the right code to use

When looking at the timeline, see figure 32 we can conclude that it took to much time to formulate a real main question for this research. Also we focused to much on finding the right values for the galactic initial conditions, which destracted from the main goal: doing simulations to discover the effect of the transverse velocity component on the merger. Though wandering off from the main subject can lead to interesting insights because one looks at the problems from a different angle, it can also be time consuming and not leading anywhere. Therefore, we recommend future students to set a fixed period for reading about the subject and then make a definite 'plan de campagne'.

7 Conclusions

Based on the computation time t_{CPU} and energy error dE, the GPU is good device to use.

88000 particles is a good number for simulations on a GPU, they have low energy errors (about 1/1000 for 500 integration time steps) and run fast (about 6 hours for 88000 particles for 500 integration timesteps) when $\eta = 3$ and $n_{crit} = 65536$ and the kirin parameter=16384. We note that setting nkirin to a higher level, comparable with n_{crit}, can possibly even lead to better performance.

For the creation of stable disks over such long timescales as proposed by this research, 44000 particles per galaxy may not be enough.

The initial conditions of the galaxy models are very uncertain. The main uncertain parameters are the halo extent and mass (dark matter distribution) and transverse velocity component.

If the transverse velocity component exceeds 171 km/s both galaxies are not bound and therefore will not merge at all.

If we want the galaxies to merge within a 'reasonable' timescale, of say 10 Giga years, the transverse velocity cannot exceed 86 km/s. The collision will happen earliest at 3.4 Gyr from now.

Chances are small but it is not impossible that there will be no collision after all.

When the galaxies do merge, they result in an elliptical galaxy.

Though the direction of the transverse velocity has no effect on the merger timescale (which is mostly determined by the halo mass) it probably will affect the shape of the merger.

Since earth will be inhabitable in about 1.1 Gyr (see section 5.3), no human (descendant) will observe Andromeda and the Milky Way to merge (at least not from earth). But the sun will stay bound to the Milky Way during the collision.

References

R. G. Abraham and S. van den Bergh. The Morphological Evolution of Galaxies. *Science*, 293:1273–1278, August 2001.

J. Barnes and P. Hut. A Hierarchical O(NlogN) Force-Calculation Algorithm. *Nature*, 324:446–449, December 1986.

R. G. Belleman, J. Bédorf, and S. F. Portegies Zwart. High performance direct gravitational N-body simulations on graphics processing units II: An implementation in CUDA. *New Astronomy*, 13:103–112, February 2008.

A. J. Benson. Self-Consistent Theory of Halo Mergers - II: CDM Power Spectra. *ArXiv e-prints*, 802, February 2008.

J. Binney and S. Tremaine. *Galactic dynamics*. Princeton, NJ, Princeton University Press, 1987, 747 p., 1987.

A. Brunthaler, M. J. Reid, H. Falcke, C. Henkel, and K. M. Menten. Proper Motions in the Andromeda Subgroup. *ArXiv e-prints*, 708, August 2007a.

A. Brunthaler, M. J. Reid, H. Falcke, C. Henkel, and K. M. Menten. The proper motion of the Local Group galaxy IC 10. *A&A*, 462:101–106, January 2007b.

D. Clowe, S. W. Randall, and M. Markevitch. Catching a bullet: direct evidence for the existence of dark matter. *Nuclear Physics B Proceedings Supplements*, 173:28–31, November 2007.

T. J. Cox and A. Loeb. The Collision Between The Milky Way And Andromeda. *ArXiv e-prints*, 705, May 2007.

W. Dehnen. A Very Fast and Momentum-conserving Tree Code. *ApJ*, 536: L39–L42, June 2000.

J. Dubinski, J. C. Mihos, and L. Hernquist. Using Tidal Tails to Probe Dark Matter Halos. *ApJ*, 462:576–+, May 1996.

N. W. Evans. Simple galaxy models with massive haloes. *MNRAS*, 260: 191–201, January 1993.

N. W. Evans and M. I. Wilkinson. The mass of the Andromeda galaxy. *MNRAS*, 316:929–942, August 2000.

K. Freeman and J. Bland-Hawthorn. The New Galaxy: Signatures of Its Formation. *ARA&A*, 40:487–537, 2002.

J. R. Gott, III and T. X. Thuan. Angular momentum in the local group. *ApJ*, 223:426–436, July 1978.

W. Herschel. On the Construction of the Heavens. *Philosophical Transactions Series I*, 75:213–266, 1785.

E. P. Hubble. A general study of diffuse galactic nebulae. *ApJ*, 56:162–199, October 1922.

E. P. Hubble. Extragalactic nebulae. *ApJ*, 64:321–369, December 1926.

E. P. Hubble. A spiral nebula as a stellar system, Messier 31. *ApJ*, 69: 103–158, March 1929.

I. D. Karachentsev and O. G. Kashibadze. Total masses of the Local Group and M 81 group derived from the local Hubble flow. *ArXiv Astrophysics e-prints*, September 2005.

J. F. Kasting. Runaway and moist greenhouse atmospheres and the evolution of earth and Venus. *Icarus*, 74:472–494, June 1988.

I. R. King. The structure of star clusters. III. Some simple dynamical models. *AJ*, 71:64–+, February 1966.

A. Koch and E. K. Grebel. The Anisotropic Distribution of M31 Satellite Galaxies: A Polar Great Plane of Early-type Companions. *AJ*, 131:1405–1415, March 2006.

K. Kuijken and J. Dubinski. Lowered Evans Models - Analytic Distribution Functions of Oblate Halo Potentials. *MNRAS*, 269:13–+, July 1994.

K. Kuijken and J. Dubinski. Nearly Self-Consistent Disc / Bulge / Halo Models for Galaxies. *MNRAS*, 277:1341–+, December 1995.

Y.-S. Li and S. D. M. White. Masses for the Local Group and the Milky Way. *MNRAS*, pages 134–+, January 2008.

A. Loeb and R. Narayan. Dynamical Constraints on the Local Group from the CMB and 2MRS Dipoles. *ArXiv e-prints*, 711, November 2007.

A. Loeb, M. J. Reid, A. Brunthaler, and H. Falcke. Constraints on the Proper Motion of the Andromeda Galaxy Based on the Survival of Its Satellite M33. *ApJ*, 633:894–898, November 2005.

M. S. Longair, editor. *Galaxy formation*, 1998.

D. Lynden-Bell. Stellar dynamics: Exact solution of the self-gravitation equation. *MNRAS*, 123:447–+, 1962.

J. Makino. A Fast Parallel Treecode with GRAPE. *PASJ*, 56:521–531, June 2004.

M. Metz, P. Kroupa, and H. Jerjen. The spatial distribution of the Milky Way and Andromeda satellite galaxies. *MNRAS*, 374:1125–1145, January 2007.

H. L. Morrison, P. Harding, K. Perrett, and D. Hurley-Keller. M31's Undisturbed Thin Disk of Globular Clusters. *ApJ*, 603:87–107, March 2004.

P. Murdin. Encyclopedia of astronomy and astrophysics. *Encyclopedia of Astronomy and Astrophysics*, 2001.

S.-M. Niemi, P. Nurmi, P. Heinämäki, and M. Valtonen. Are the nearby groups of galaxies gravitationally bound objects? *MNRAS*, 382:1864–1876, December 2007.

E. Opik. An estimate of the distance of the Andromeda Nebula. *ApJ*, 55: 406–410, June 1922.

J. P. Ostriker and P. J. E. Peebles. A Numerical Study of the Stability of Flattened Galaxies: or, can Cold Galaxies Survive? *ApJ*, 186:467–480, December 1973.

J. S. Plaskett. The Structure and Rotation of the Galaxy. *PASP*, 44:141–+, June 1932.

S. F. Portegies Zwart, R. G. Belleman, and P. M. Geldof. High-performance direct gravitational N-body simulations on graphics processing units. *New Astronomy*, 12:641–650, November 2007.

H.-J. Seo, D. J. Eisenstein, and I. Zehavi. Passive Evolution of Galaxy Clustering. *ArXiv e-prints*, 712, December 2007.

L.S. Sparke and J.S. Gallager. Cambride University Press, 2000.

B. M. Tinsley and R. B. Larson, editors. *Evolution of galaxies and stellar populations*, 1977.

A. Toomre. Some flattened isothermal models of galaxies. *ApJ*, 259:535–543, August 1982.

R. P. van der Marel and P. Guhathakurta. M31 Transverse Velocity and Local Group Mass from Satellite Kinematics. *ArXiv e-prints*, 709, September 2007.

L. M. Widrow and J. Dubinski. Equilibrium Disk-Bulge-Halo Models for the Milky Way and Andromeda Galaxies. *ApJ*, 631:838–855, October 2005.

L. M. Widrow, K. M. Perrett, and S. H. Suyu. Disk-Bulge-Halo Models for the Andromeda Galaxy. *ApJ*, 588:311–325, May 2003.

Parameter	M31	MW
Orientation spin axis (l, b)	(240,-30)	(0,-90)
Distance (kpc)	780	8.5
Position (kpc)	(-369.8, 615.4, -304.8)	(-8.5,0,0)
Mass total ($\times 10^{11} M_{\odot}$)	19.5	19.5
Mass disk	0.42	0.42
Mass bulge	0.22	0.22
Mass halo	18.9	18.9
Radial velocity (km/s)	117	-
Transverse velocity	≤ 171	-
Relative velocity	$117 \leq v_t \leq 207$	-

Table 9: Input parameters

A Input parameters

Kuijken and Dubinski (1995) use a unit mass of 5.1 10^{10} $M_{\odot}$, a unit length of $R_d = 4.5kpc$, and a unit velocity of v=220 km/s. With G=1, this corresponds to a natural unit of time of $t = 20\ 10^6 year$. Tables 9 and 10 give an overview of the used parameters.

B Coordinates

Galactic or heliocentric coordinate systems have the sun or the earth as its centre, figure 33, with the x-axis pointing to the Galactic centre. The longitude l is the anticlockwise angle measured from the x-axis between 0° and 360°. The lattitude b is the heigth above the plane, between $-90°$ (negative z-axis) and 90° (positive z-axis).

C Paper by Widrow et al.

Widrow et al. (2003) use the K&D-model to create a model for Andromeda that best fits the observed rotation curve, surface brightness profile and the bulge velocity profiles. Their used physical units differ from Kuijken and Dubinski (1995): Mass: 2.325 10^{+9} $M_{\odot}$[11], length: 1 kpc, velocity:100 km/s, G=1. With a multidimensional minimization technique they come up with a model that best fits the observed profiles. Initially, we decided to use one of these best fit models. Using their input parameters we created a model that had a good fit to the observed rotation curve, see figure 34. Unfortunately our model did not reproduce their masses and mass ratios (see Widrow et al.

[10]Ignoring the effects of the distribution function truncation.

[11]Typing error in (Widrow et al., 2003): minus sign on page 325 should be plus sign.

Parameter	**K&D** model D
Disk	
Mass M_d	0.867
Scale length R_d	1
Outer/truncation radius R_{outer}	5
Scale height z_d	0.1
Truncation width δR_{trunc}	0.5
Bulge	
Central density ρ_b	14.45
Velocity dispersion/central potential σ_b	0.714
Cut-off potential[10] Ψ_c	-4.7
Halo	
Central potential Ψ_0	-7
Central velocity v_0 $(= \sqrt{2}\sigma_0)$	1.3
Flattening parameter q	1
Core smoothing parameter $(\frac{R_c}{R_k})^2$	0.1
Scaling radius R_a	0.8
Potential	
Width radial bin δr	0.01
Number of radial bins nr	7500
Largest value potential harmonic expansion l_{max}	10

Table 10: Input parameters in K&D-units

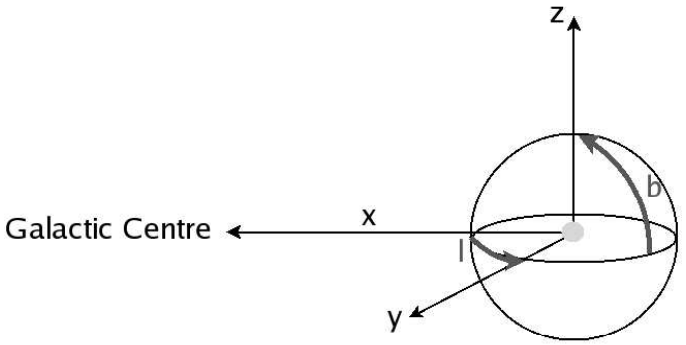

Figure 33: Galactic/heliocentric coordinates with longitude $0° < l < 360°$ (lies in the plane of the galaxy), and lattitude $-90° < b < 90°$ (the height above the plane). The x-axis points to the Galactic centre. Galactic coordinates take the Galactic centre as centre and heliocentric coordinates take the sun as centre.

(2003), table 1). A possible reason for this is that they use a slightly different version of the GalactICS program.

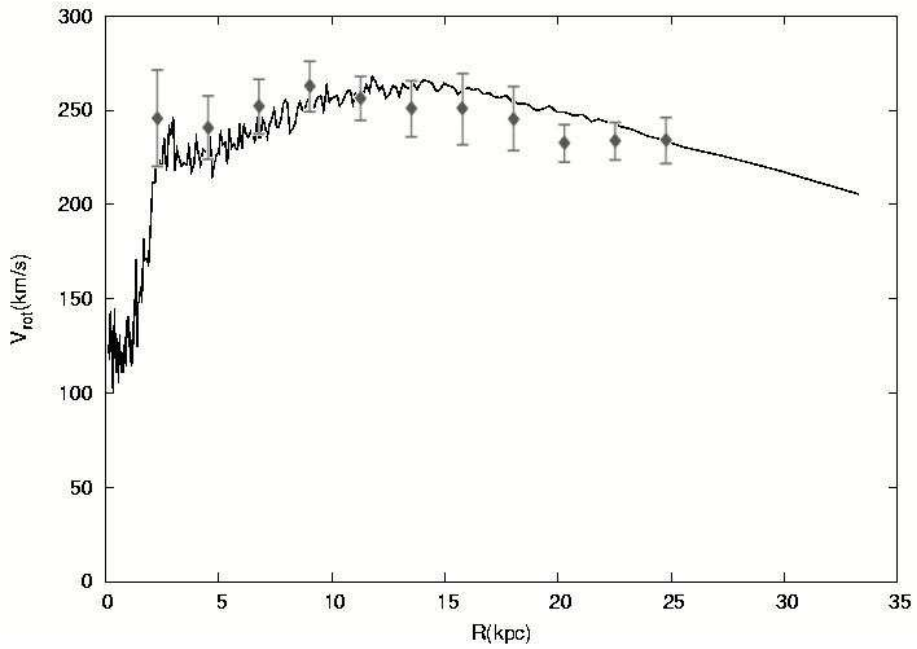

Figure 34: The rotation curve created using the model input parameters of Widrow et al. (2003), plotted with error according to Widrow et al. (2003).

Samenvatting

Op een heldere avond kun je een witte band van sterren aan de hemel zien, de Melkweg. Deze sterren samen vormen een sterrenstelsel die als een platte schijf ronddraait, en wij maken daar deel van uit. Er zijn verschillende soorten sterrenstelsels. Hubble ontwierp een classificatiesysteem voor deze stelsels, gebaseerd op vorm. Grofweg kun je de stelsels opdelen in Diskstelsels (met of zonder spiraalarmen) en Elliptische Stelsels. Voor dit onderzoek is nog een type stelsel belangrijk: de 'Eigenaardige' Stelsels (Peculiar Galaxies). Dit zijn systemen die niet binnen de andere categorieën vallen, vanwege hun vreemde vorm. Dit eigenaardige type bestaat uit twee botsende stelsels. De huidige (geaccepteerde) theorie is dat twee botsende Spiraalstelsels resulteren in één groot Elliptisch Stelsel, tijdens de botsing noemt men het stelsel 'Eigenaardig'.

Andromeda is, net als de Melkweg, een spiraal stelsel, en samen met enkele kleinere sterrenstelsels vormen we de lokale groep. Andromeda staat ver van ons af, ongeveer 780 kpc, dat is ongeveer 2.5 miljoen lichtjaar. We meten door middel van roodverschuiving dat Andromeda met 117 km/s in onze richting beweegt. Dus het lijkt er op dat ons een enorme botsing te wachten staat, dit wordt algemeen aangenomen in de sterrenkunde.

Toch is er een kans dat we niet botsen. De snelheid van Andromeda loodrecht op de Melkweg (transversale snelheid) is namelijk onbekend. Andromeda staat zo ver weg, dat het niet mogelijk is deze beweging direct waar te nemen. Als deze transversale snelheid maar hoog genoeg is, schieten we langs elkaar heen. Dit onderzoek richt zich op de vraag of het mogelijk is dat er geen botsing plaats zal vinden tussen Andromeda en de Melkweg.

Er bestaan verschillende methodes om een schatting te maken van de transversale snelheid. Wij gebruiken de aanname dat Andromeda en de Melkweg gebonden zijn, dus dat hun relatieve beweging bepaald wordt door elkaars zwaartekracht. Wanneer we de stelsels benaderen als puntmassa's, vinden we zo een maximale transversale snelheid van 171 km/s. Andere schattingen variëren van nul tot tweehonderd kilometer per seconde.

Om uit te zoeken of er een kans is dat er geen botsing zal plaatsvinden, hebben we een simulatie gemaakt van beide stelsels, waarin we kijken naar de ontwikkeling van het Andromeda-Melkweg systeem in de tijd, en wat het effect is van de transversale snelheid.

Om onze simulaties, met 88000 deeltjes, zo snel mogelijk te laten verlopen, hebben we verschillende numerieke methoden met elkaar vergeleken. Uiteindelijk kozen we, op basis van lage foutenmarges in de energie en vanwege

een snelle rekentijd, voor een methode die niet op een normale PC wordt uitgevoerd, maar op een GPU (Graphical Processing Unit). Deze processor zit op de grafische kaart van een computer en verwerkt normaal gesproken de beelden om ze te representeren op het scherm. In ons geval is de GPU zo geprogrammeerd dat hij heel snel voor veel deeltjes de onderlinge krachten kan uitrekenen.

Met behulp van de simulaties kwamen we er achter dat de Melkweg op zijn vroegst over 3,4 miljard jaar gaat botsen met Andromeda. Mocht de transversale snelheid groter zijn dan 171 km/s dan botsen beide stelsels helemaal niet. Onze simulaties laten zien dat er weinig vreemde structuren worden gevormd, die zo typisch zijn voor Eigenaardige Stelsels. Bovendien merken we dat de transversale snelheid invloed heeft op de uiteindelijke vorm van het elliptische stelsel.

Onze resultaten wijken enigszins af van eerder onderzoek, maar de verschillen zijn te verklaren door het gebruik van andere aannames en beginvoorwaarden. Zo nemen wij in onze simulaties geen gas mee, dit heeft invloed op de vorming van vreemde structuren. Bovendien is de transversale snelheid niet de enige onzekere waarde, ook de schattingen voor de massa en de grootte van de stelsels lopen zeer uiteen. Dit komt omdat de sterrenstelsels omringd worden door een onbekende massa, donkere materie, die we niet kunnen zien. De totale massa van beide stelsels wordt voor het grootste gedeelte bepaald door deze donkere materie. Om met meer zekerheid te kunnen zeggen of er een botsing gaat plaatsvinden en op welke tijdschaal, zal er nog veel onderzoek gedaan moeten worden.

Acknowledgements

I would like to thank everybody that supported me while doing this research and writing this thesis. First of all I thank Simon Portegies Zwart for giving me the opportunity to do this exciting project, and for his enthusiastic supervision. Simon, thank you for responding to all my PANIC!!!-mail, even on weekends. Second, many thanks go to Stefan Harfst. Stefan, I really felt you always had time for me and I could ask you anything - at least when you were not hiding behind the door ;)
Also I would like to thank everyone of the N-body group, especially Atakan, Derek, Evghenii and Johan, for useful comments and interesting group meetings.
With this thesis I do not only say goodbye to Andromeda, but also to the API. I had a wonderful time there. So I want to thank all API's for making it such a good place to work *and* relax. Special thanks to all students of 'studentenkamer 1', and please take good care of the ficus.
Of course I also thank my parents, sister and Guillermo. You really helped me through the last weeks of my project.

Lyrics Enigma- Goodbye Milky Way

Shall I go, shall I stay
107 light years away
Many times, so many doubts
But no reason to talk about

Mission is over, mission is done
I will miss you, children of the sun
Now it's time to go away
Goodbye, goodbye Milky Way

For a better world without hate
Follow your heart, believe in fate
Only visions and the mind
Will guide you to the light

Mission is over mission is done
I will miss you children of the sun
Now it's time to go and say
Goodbye, goodbye Milky Way

Mission is over, mission is done
I will miss you children of the sun
I go home until someday
I say goodbye, goodbye Milky Way

In 5 billions years the Andromeda galaxy will collide with our Milky Way
A new gigantic Cosmic world will be born